“Targeting the AKT Pathway in Glioblastoma Multiforme”

Md Abdul Latif

This thesis is submitted in partial fulfilment of the requirements for the degree of Master in Medical Cell Biology – “[2014-2016]’’

Department of Biomedicine

University of Bergen

June, 2016

Acknowledgements

I express my indebtedness, sincere appreciation to Dr. Lars Prestegarden, Researcher of the Department of Biomedicine, University of Bergen, Norway for his constant supervision, valuable suggestion, scholastic guidance for conducting the research and writing this manuscript.

I express my gratefulness and gratitude to my reverent research co-supervisor Mr. Mahdi Hasan, PhD fellow of the Department of Biomedicine, University of Bergen, Norway for his kind co-operation, valuable advice, continuous inspiration, and factual comments during the research work and writing this manuscript.

I am very grateful and sincerely wish to express my respect to Dr. Rolf Bjerkvig, Professor, and Group Leader of "Translational Cancer Research" of the Department of Biomedicine, University of Bergen, Norway for allowing me to pursue the thesis work in his group.

Cordial thanks to my lab fellows Dr. Justin Vareecal Joseph, Dr. Lina Wik Leiss, Andrea Gras Navarro, Rajib Chaulagain and Jubayer Hossain for your continuous help, inspiration, and kind co-operation during the period of thesis work. Thanks to Bodil, Tove and Halala for your help in the lab.

Great thanks to Dr. Hrvoje Miletic, Dr. Martha Chekenya Enger, Dr. Marit Bakke, Dr. Frits Alan Thorsen, Dr. Stein Ove Døskeland and all of my respective faculty members for delivering cutting edge lectures during the study period.

Thanks to all of my friends especially Nasreen, Shahin, Hymonti, Linn, Mia and Kunwar for being a part of my daily life.

Finally, I acknowledge my gratitude and profound respect to my beloved parents, elder sisters and all other relatives for their blessings and inspirations.

Latif, May 2016

Contents

List of Tables

List of Figures

Abbreviations

Abbreviation	Full name
ATP	Adenosine triphosphate
ATG13	Autophagy-related protein-13
BCA	Bicinchoninic acid
CCD	Charged couple device
CDKN2A	Cyclin-dependent kinase inhibitor-2A
CNS	Central nervous system
DAPI	4,6-diamidino-2-phenylindole
DMEM	Dulbeccos modified eagles medium
DMSO	Dimethyl sulphoxide
DNA	Deoxyribonucleic acid
DNAPK	DNA-dependent protein kinase
ECL	Enhanced chemiluminescence
EGFR	Epidermal growth factor receptor
FITC	Fluorescein isothiocyanate
FOXO	Forkhead box O
GBM	Glioblastoma multiforme
GF	Growth factor
GSK	Glycogen synthase kinase
HKPs	Housekeeping proteins
HRP	Horseradish peroxidase
HM	Hydrophobic motif
IDH	Isocitrate dehydrogenase
IRS	Insulin receptor substrate
LOH	Loss of heterozygosity
MDM2	Mouse double minute-2 homolog
MMP9	Matrix metalloproteinase-9
mTORC	Mammalian target of rapamycin complex
MTS	(3-(4,5-dimethylthiazol-2-yl)-5-(3-carboxymethoxyphenyl)-2-(4-sulfophenyl)-2H-tetrazolium)
MTT	(3-(4,5-dimethylthiazol-2-yl)-2,5-diphenyltetrazolium bromide)
NaCl	Sodium chloride
NEAA	Non-essential amino acid
PAGE	Polyacrylamide gel electrophoresis
PBS	Dulbeccos phosphate-buffered saline
PBST	Dulbeccos phosphate-buffered saline Tween-20
PDK1	Phosphoinositide dependent protein kinase-1
PH	Pleckstrin homology
PHLPP	PH-domain and leucine rich repeat protein phosphatase
PI3K	Phosphoinositide 3-kinase
PIP2	Phosphatidylinositol (3,4)-bisphosphate
PIP3	Phosphatidylinositol (3,4,5)-trisphosphate
PKB	Protein kinase B
PMT	Photomultiplier tube

PP2A	Protein phosphatase 2A
PRAS40	The proline-rich AKT substrate of 40 kDa
PTEN	Phosphatase and tensin homolog
RIPA	Radio immunoprecipitation assay buffer
SD	Standard deviation
TP53	Tumour protein p53
TSC	Tuberous sclerosis proteins
ULK1	Unc-51 like autophagy activating kinase-1
wt%	Weight percent
w/v	Weight per volume

Summary

Background: Glioblastoma multiforme (GBM) is the most common primary brain tumour with dismal prognosis. GBMs are heterogenous tumours hence the name multiforme. The heterogeneity is reflected in histology, clinical presentation and genetic signature. The incidence of GBM is less than 10 to 100,000 but it accounts for 12-15% of all brain tumours. Exposure to ionizing radiation is the only known risk factor for developing glioma; there is no significant association reported with smoking, cellular phones, electromagnetic fields or diet. In GBM, the phosphoinositide 3-kinase/AKT (PI3K/AKT) pathway is dysregulated in about 89.6% of tumours and leads to increased activity in the protein kinase AKT. AKT promotes proliferation, cell survival and resistance to chemotherapy by regulation of various downstream effectors. Several AKT inhibitors are currently in clinical trials for different cancer types. However, the specific role of AKT inhibitors for GBM treatment is yet to be determined.

In this study, allosteric and adenosine triphosphate (ATP) competitive kinase inhibitors of AKT were investigated in SKMG-3 (epidermal growth factor receptor (EGFR)-amplified; phosphatase and tensin homolog (PTEN)-null) and U-87 (EGFR-low, PTEN-null) GBM cell lines. It has been hypothesized that AKT inhibitors will induce cell death in GBM cell lines by blocking AKT activity. As such this project aims to investigate the effects of AKT inhibitors *in vitro*, determine the effects of AKT inhibitors on the clonogenic capacity and elucidate the cellular death mechanism induced by AKT inhibition.

Methods: The cytotoxic effects of the drugs were determined by the cell viability assay based on cellular enzymatic activity. The antiproliferative effect of the AKT inhibitors was investigated by clonogenic assay. Western blot analysis was performed to evaluate the levels of apoptotic markers and phosphorylation status of downstream AKT substrates. Expression of phospho-AKT (Serine473) was visualized by immunofluorescence microscopy.

Results: Among the inhibitors included in this study, MK-2206 and GSK-2141795 demonstrated superior therapeutic efficacy in both GBM cell lines. However, the EGFR amplified SKMG-3 cell line was much more sensitive to AKT inhibitors compared to the U-87 cell line. The clonogenic potential of SKMG-3 cells was completely inhibited while some colonies of the U-87

cells survived in the given therapeutic regime. Cells treated with either compound showed decreased phosphorylation of the downstream substrate of AKT. This induced rapid apoptosis in SKMG-3 cells; however, apoptosis was not detectable upon AKT inhibition in U-87 cells.

Conclusion and future perspectives: The results reported in this study indicate that AKT inhibitors should be further studied *in vivo* with a particular focus on the EGFR amplified subgroup. These AKT inhibitors can potentially be tested as a combinational therapy with EGFR inhibitors for achieving synergistic effects of the drugs and to overcome the drug resistance in EGFR amplified GBM. Moreover, targeting specific pathways may reduce adverse drug side effects. In future studies a panel of normal human astrocyte cell lines will be tested *in vitro* to assess the potential toxicity of these AKT inhibitors either as a mono or combinational therapy.

Chapter 1
Introduction

1.1 Glioblastoma multiforme (GBM)

GBM tumours are usually highly malignant, rapidly progressive astrocytoma with a median survival of 14-15 months (Stupp *et al*., 2005). The name GBM was first introduced by Mallory in 1914 due to the heterogenous nature of these tumours. As the incidence is fairly constant globally it is unlikely that environmental and geographical factors play a major role in the pathogenesis of GBM. Common clinical symptoms are dysphagia, seizures, headaches, cognitive changes, eye weakness and vomiting (Oberndorfer *et al*., 2008; Eefje *et al*., 2010). Progression of high intracranial pressure is one of the most dangerous features of GBM (Oberndorfer *et al*., 2008; Pace *et al*., 2009).

The incidence of GBM increases with age with a peak at 58 years. About 8.8% of children with central nervous system tumours have GBM (Dohrmann *et al*., 1976) and congenital cases are rare. Men are more prone to GBM slightly more than women, with a ratio of 3:2. The reason for this gender distribution is unknown (Iacob and Dinca, 2009). Gliomas usually appear sporadically but several genetic disorders are associated with increased incidence, including neurofibromatosis type-1 and type-2, Li–Fraumeni syndromes, von Hippel Lindau disease (Iacob and Dinca, 2009).

The location of the tumour within the brain is variable (Holland, 2000). However, tumour cells are usually aggregated in the cerebral hemispheres with occasionally contralateral invasion and in association to the basal ganglia and lateral ventricles (Figure 1) (Lim *et al*., 2007).

Depending on the cell of origin, gliomas can be divided into three subtypes: oligodendrogliomas, ependymomas and astrocytomas. Astrocytomas originate from astrocytes and invade through the normal brain tissue, which make it incurable by surgery. Around 35% of all brain tumours are astrocytomas which are histologically classified as low, intermediate or high grade. The highest grade of astrocytoma is called GBM.

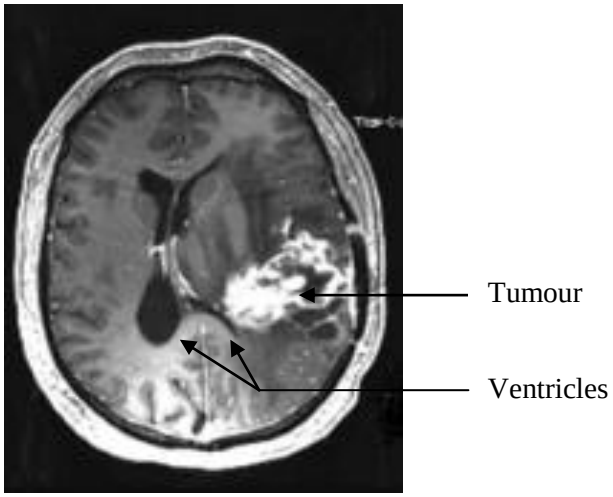

Figure 1: Localization of GBM. Magnetic Resonance Image (MRI) showing a GBM as a contrast enhanced tumour in association with the lateral ventricle (Benedikte *et al*., 2010).

The current standard care for GBM includes debulking surgery with focal fractionated radiotherapy with concomitant chemotherapy with Temozolomide. Aberration in oncogenic signaling pathways, diversity of mutated genes, tumour microenvironment and pathological angiogenesis are key prioritized areas in GBM. Several GBM candidate cancer genes (CAN-genes) have been associated with GBM pathogenesis (Table 1). New targeted therapeutic approaches including inhibitors of growth factors and their receptors, intracellular signaling pathways and tumour angiogenesis are under investigation. For example, bevacizumab, an anti-angiogenic agent has been shown a significant effect for treatment of recurrent GBM (Kreisl *et al*., 2009). However, the effect on overall survival did not reach statistical significance (Moller *et al*., 2012; Patel *et al*., 2012).

1.2 Genetic aberrations in GBM

Primary GBM: Primary GBMs arise as *de novo* that account for 95% of all GBM (Ohgaki and Kleihues, 2005). EGFR is frequently amplified in primary GBM (Kunihiko *et al*., 2008). In addition to EGFR over expression, PTEN mutations, cyclin-dependent kinase inhibitor-2A (CDKN2A) deletions and less frequently mouse double minute-2 homolog (MDM2) amplification are associated with primary GBM (Paul and Hiroko, 1999).

Table 1: Candidate cancer genes (CAN-genes) in GBM pathogenesis

CAN-genes	Proportion of alterations (%)	References
Catalytic subunit of phosphatidylinositol-3-kinase (PIK3CA)	8 to 10	Mizoguchi *et al*., 2004; Parsons *et al*., 2008
Cyclin-dependent kinase inhibitor-2A (CDKN2A)	50	Albert *et al*., 1987; Parsons *et al*., 2008
Epidermal growth factor receptor (EGFR)	30 to 40	Albert *et al*., 1987; Parsons *et al*., 2008
Phosphatase and tensin homolog (PTEN)	30 to 40	Li *et al*., 1997; Parsons *et al*., 2008
Neurofibromatosis type-1 (NF1)	12 to 15	Mizoguchi *et al*., 2004; Parsons *et al*., 2008
Retinoblastoma protein-1 (RB1)	12 to 15	Albert *et al*., 1987; Parsons *et al*., 2008
Regulatory subunit of phosphatidylinositol-3-kinase (PIK3R1)	8 to 10	Mizoguchi *et al*., 2004; Parsons *et al*., 2008
Tumour protein p53 (TP53)	30 to 40	Janice *et al*., 1989; Parsons *et al*., 2008

Secondary GBM: Secondary GBMs arise from lower grade gliomas that constitute 5% of GBMs and mostly younger patients are affected (Ohgaki and Kleihues, 2005). Isocitrate dehydrogenase (IDH1) mutations are the earliest detectable precursor in low-grade diffuse astrocytomas and in oligodendrogliomas (Ohgaki and Kleihues, 2013). TP53 mutations occur with a high frequency in secondary GBM (Kunihiko *et al*., 2008).

Common mutations: Loss of heterozygosity (LOH) mutation is the most common genetic alteration on the long arm of chromosome 10 and occurs in about 60 to 80% of both primary and secondary GBM (Ohgaki and Kleihues, 2007).

1.3 Current histopathological classification

Histopathological classification is based solely on morphology. Primary and secondary GBM show similar characteristics histologically but vary in their genetic and epigenetic profiles. Malignant diffuse gliomas include oligodendroglioma, astrocytoma and heterogeneous oligoastrocytic neoplasms (Louis *et al*., 2007). They are preferentially located in the frontal lobe and carry a significantly better prognosis and exert a lesser degree of necrosis (Ohgaki and Kleihues, 2013). Grade-I gliomas are characterized by low proliferative potential and are often

cured following surgical resection. Grade-II gliomas are generally infiltrative in nature and have a tendency to recur. Grade-III GBMs are characterized by nuclear atypia and mitotic activity. In most cases, patients of grade-III gliomas receive adjuvant radiation and/or chemotherapy. Pseudopalisading necrosis and/or microvascular proliferation is a characteristic for grade-IV astrocytoma (Miller and Perry, 2007). Grade-III and grade-IV tumours together comprise the clinical entity termed "malignant glioma" (Dunn *et al*., 2012).

1.4 Tumour grades as prognostic factor

Tumour grades I-IV are used to predict a response to therapy and outcome. Several parameters are considered to estimate the overall prognosis of each tumour entity such as the clinical findings (age of the patient, neurologic performance status and location of the tumour), radiological features (proliferation indices, extent of surgical resection) and genetic alterations. Patients with grade-II tumours typically survive more than 5 years but those with grade-III tumours survive 2–3 years (Louis *et al*., 2007). The overall survival is poor independent of treatment with grade-IV tumours (GBM).

1.5 Regulation of AKT

The PI3K/AKT signaling pathway is very crucial for maintaining many normal cellular functions. In GBM, the PI3K/AKT pathway is commonly deregulated. AKT is a master regulator in this pathway and belongs to the AGC protein kinase family. The term AGC kinase was proposed in 1995 to define the subgroup of Serine/Threonine protein kinases that are based on sequence homology of their catalytic kinase domain (Hanks and Hunter, 1995). The three isoforms of AKT are AKT1, AKT2, and AKT3. These multi-domain containing isoforms are highly homologous and contain an amino (N) terminal pleckstrin homology (PH) domain, inter domain linker, kinase domain and carboxy (C) terminal hydrophobic motif (HM) (Yang *et al*., 2002; Kannan *et al*., 2007). These isoforms possess both common and distinct cellular functions. In normal cells, AKT regulates metabolism, growth, proliferation, differentiation and survival (Brazil *et al*., 2004; Carnero, 2010). Similar effects are identified for cancer cells where AKT in addition promotes resistance to cancer chemotherapy or radiotherapy (Winograd-Katz and Levitzki, 2006; Rao *et al*., 2012).

In this study, allosteric (MK-2206) and ATP competitive kinase inhibitors (GSK-2141795, GDC-0068, and GSK-690693) of AKT were investigated in two GBM cell lines, SKMG-3 and U-87. In the cell survival assay, MK-2206 and GSK-2141795 inhibitors demonstrated potent therapeutic efficacy in both cell lines. As such, these two inhibitors were used for the subsequent studies.

PI3K/AKT pathway is regulated by a multistep process. The inactive form of AKT is termed the closed or 'PH-in' conformation (Wen *et al*., 2010) in which the PH domain interacts extensively with the kinase domain. Residues of the PH domain and ATP binding site are involved in inter domain interactions. AKT stays in a 'PH-in' conformation before being translocated and phosphorylated (Calleja *et al*., 2009). Upon receptor activation, adapter molecules such as the insulin receptor substrate (IRS) proteins bind to the receptor. This triggers activation of PI3K by interacting of its regulatory subunit with the bound adapter molecules. The catalytic domain of PI3K transforms phosphatidylinositol (3,4)-bisphosphate (PIP2) to phosphatidylinositol (3,4,5)-trisphosphate (PIP3). AKT kinases are bound to PIP3 lipids through PH domain. This translocation allows phosphorylation at threonine 308 (Thr308) by phosphoinositide dependent protein kinase-1 (PDK1) that causes partial activation of AKT (Alessi *et al*., 1997). Full activation of AKT requires phosphorylation at Serine 473 (Ser473) in the carboxy-terminal hydrophobic motif, either by DNA-dependent protein kinase (DNAPK) (Feng *et al*., 2004) or mammalian target of rapamycin complex-2 (mTORC2) (Sarbassov *et al*., 2005) (Figure 2). To phosphorylate the downstream substrates of AKT, ATP must be localized in the ATP binding pocket of an activated AKT. Binding of ATP protects AKT from dephosphorylation until ATP is hydrolyzed into adenosine diphosphate (ADP), upon which a conformational change occurs that promotes the dephosphorylation and inactivation of AKT (Kui *et al*., 2012). Activation of AKT leads to phosphorylation of a variety of proteins, forkhead box O (FOXO), tuberous sclerosis proteins (TSC1/2), proline-rich AKT substrate of 40 kDa (PRAS40), glycogen synthase kinase (GSK3β) etc (Brendan and Lewis, 2007). Dephosphorylation of Thr308 by protein phosphatase 2A (PP2A); Ser473 by PH-domain and leucine rich repeat protein phosphatase (PHLPP1/2) and the conversion of PIP3 to PIP2 by PTEN antagonize AKT signaling (Andjelkovic *et al*., 1996; Stambolic *et al*., 1998; Brognard *et al*., 2007).

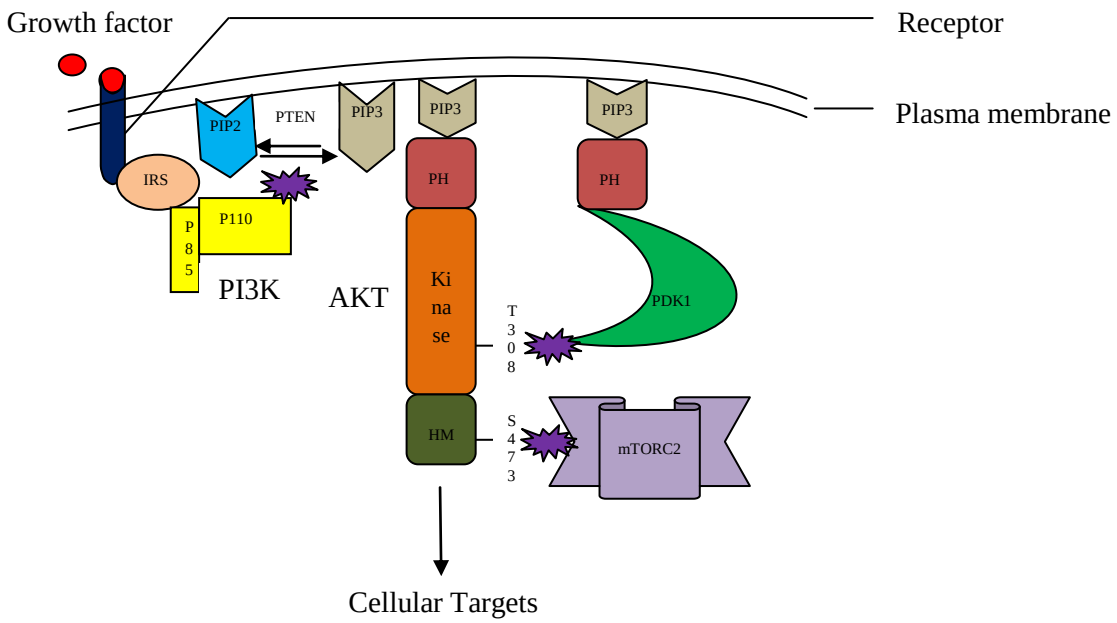

Figure 2: Molecular mechanism of AKT activation. Interaction of a growth factor to the receptor allows binding of the adaptor molecules (IRS) to the receptor. This binding triggers PI3K activation that converts PIP2 to PIP3. AKT and PDK are bound to PIP3 by PH domain. Complete activation of AKT requires phosphorylation at Thr308 (T308) and Ser473 (S473) by PDK and mTORC2 respectively (Modified from Ronald *et al*., 2009).

1.6 Mechanism of ATP competitive inhibitors

Incubating cells with ATP competitive inhibitors of AKT induce hyperphosphorylation of Thr308 and Ser473 residues. These inhibitors mimic ATP and show higher binding affinity to the AKT binding site of an activated AKT (Wen *et al*., 2010). All AKT protein kinases have a similar protein fold that consists of two lobes: N-terminal lobe consists of mainly β-sheet structure and the C-terminal lobe consists of α-helices. This lobe structure creates an ATP-binding cleft that constitutes the active site (Jeffrey and James, 2007). Activated AKT undergoes a substantial conformational change which renders phosphorylated sites inaccessible to phosphatases. Inhibitors bind to the ATP binding site of the AKT and appear to restrict intra and inter domain movement through their extensive contacts with residues in both lobes. In inhibited AKT, the phosphate group of Ser473 forms intra molecular interactions with Aspartic acid (Asp) while the phosphate group of Thr308 forms intra molecular interactions with Arginine (Arg273)

and Lysine (Lys297). These interactions are positioned close to the main surface of the kinase and do not protrude from the surface in an extended conformation, thus limiting the accessibility to phosphatases. In inactivated AKT, Tyrosine (Tyr229) is rotated into the ATP binding pocket, resisting binding of nucleotides or ATP competitive inhibitors. In addition, Phenylalanine (Phe293) exerts steric hindrance for inhibitor's binding to the inactive, DFG (Asp-Phe-Gly)-out loop conformation (Kui *et al*., 2012). However, the PH domain cannot remain fully closed onto the kinase domain when ATP competitive inhibitors occupy the ATP binding site. Thus the phospholipid binding site of AKT becomes exposed which may increase the propensity of AKT to localize in the membrane (Wen *et al*., 2010).

1.6.1 GSK-690693

GSK-690693 (Figure 3) is an ATP competitive pan-AKT (Total AKT) kinase inhibitor. *In vitro* and *in vivo* studies of GSK-690693 in different cancer types have demonstrated that this compound inhibits AKT, and increases apoptosis (Deborah *et al*., 2010).

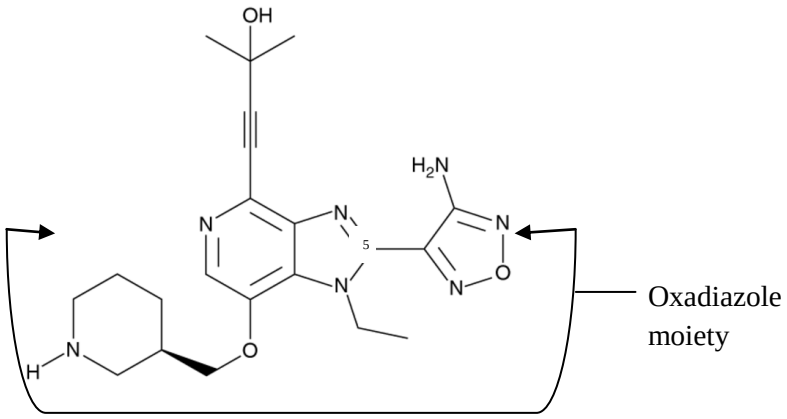

Figure 3: **Chemical structure of GSK-690693**. The compound binds to the ATP binding pocket of AKT by making a key hydrogen bonding contact between N-5 of the oxadiazole moiety and the backbone NH of Alanine (Ala232) in the hinge-binding region. The hydrogen bonding network between the backbone NH of Phe294 and the side chain carboxylic acid of Glutamic acid (Glu200) with the alkynol-OH is another important interaction (Dirk *et al*., 2008).

1.6.2 GDC-0068

GDC-0068 (Figure 4) is an orally bioavailable and potent pan-AKT inhibitor that can inhibit all three AKT isoforms. It demonstrates decreased viability of cancer cell lines and proficient antitumour response in xenograft models, resulting in the blockade of cell cycle progression (James *et al*., 2012; Lin *et al*., 2013). This compound is currently under evaluation in several clinical phase-I and II trials for the treatment of various human cancers including metastatic triple-negative breast cancer (Kim *et al*., 2015).

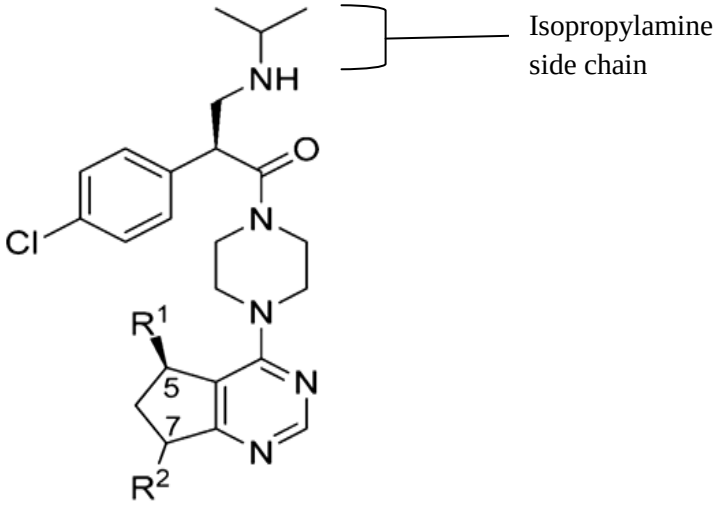

Figure 4: Chemical structure of GDC-0068. The isopropylamine side chain interacts in the carbonyl rich region with the carboxylate side chains of Glu234 and Glu278. Pyrimidine ring of GDC-0068 interacts via a hydrogen bond to the amide NH of Ala230 in the hinge region of AKT. Target side chain of Ala230 in AKT creates a pocket that enables substitution of the GDC-0068 core with various groups that afford a high degree of selectivity to AKT (James *et al*., 2012).

1.6.3 GSK-2141795

GSK-2141795 (Figure 5) is orally bioavailable, and a potent ATP competitive inhibitor of all AKT isoforms. Preclinical studies had demonstrated that this compound inhibited proliferation of cancer cell lines. GSK-2141795 treatment decreases phosphorylation of downstream substrates of AKT. Consistent with AKT pathway inhibition *in vitro*, treatment of tumour bearing mice

with GSK-2141795 resulted in tumour growth inhibition and regression (Melissa *et al*., 2014). A phase-I study showed that this compound was well tolerated with reversible and predictable toxicities (Burris *et al*., 2011).

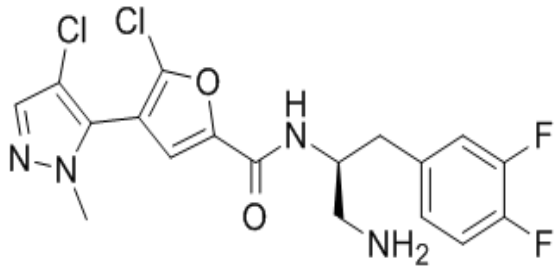

Figure 5: Chemical structure of GSK-2141795. The compound binds to various residues of the ATP binding pocket of AKT (Dumble *et al*., 2014).

1.7 Mechanism of allosteric inhibitors

Generally, allosteric inhibitors bind to Tryptophan (Trp80) of the 'PH-in' conformation of AKT (Wen *et al*., 2010). These inhibitors inhibit both membrane association and activation of AKT (Barnett *et al*., 2005; Calleja *et al*., 2009). Mechanistically, they lock AKT into a closed conformation. In closed conformation, phospholipid binding site is blocked by the kinase domain. As a result, allosterically inhibited AKT remains cytosolic (Wen *et al*., 2010). As such, the loss of AKT conformational change upon inhibitor's binding explains the loss of Thr308 phosphorylation but is not a fully satisfactory explanation for the loss of Ser473 phosphorylation in the HM site. Loss of Ser473 phosphorylation may occur in two possible ways. First, binding of the inhibitors can lead to an incorrect positioning of the HM which may cause increased Ser473 dephosphorylation by phosphatases (Wen *et al*., 2010). Second, binding of inhibitors can create a steric hindrance that prevents the upstream kinase(s) from phosphorylating Ser473 (Calleja *et al*., 2009).

1.7.1 MK-2206

MK-2206 (Figure 6) is an allosteric AKT inhibitor that is orally ingested. It inhibits all three forms of AKT but has a higher affinity for AKT1 by interaction with Trp80 of the pleckstrin-homology domain (Mohd *et al*., 2014). This allosteric AKT inhibitor locks AKT in a closed

conformation with its phospholipid binding site blocked by the kinase domain thus inhibiting its subsequent activation (Wen *et al*., 2010; Liu *et al*., 2011; Knowles *et al*., 2011; Ma *et al*., 2013). MK-2206 has demonstrated preclinical efficacy in several cancer types (Meng *et al*., 2010; Hirai *et al*., 2010; Balasis *et al*., 2011) by inducing apoptosis (Cheng *et al*., 2012). MK-2206 at a dose of 135 mg/week is safe and well tolerated (Chien *et al*., 2016).

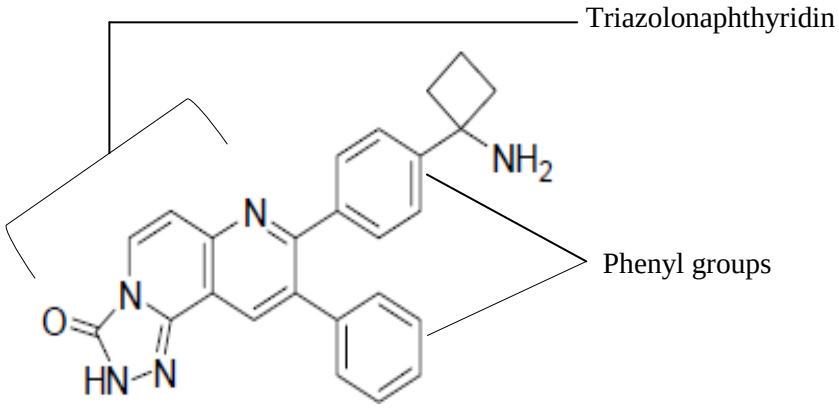

Figure 6: Chemical structure of MK-2206. The two phenyl groups protruding from triazolonaphthyridin moiety bind with different residues especially with Trp80 within the allosteric site of AKT (Mohd *et al*., 2014).

1.8 Cancer cell line as an *in vitro* model system to study cancer

In vitro cancer models have offered great insights into cellular pathways and mechanisms involved in cancer cell biology (Gazdar *et al*., 2010). Cell lines usually provide the first proof-of-principle for identifying new therapeutic targets. Since they harbor the essential cancer cell features such as an abnormal karyotype, uncontrolled proliferation, clonogenicity etc. The "Cancer Cell Line Encyclopedia" has compiled the molecular profiles of a large panel of human cancer cell lines (Barretina *et al*., 2012), and these profiles can be compared to a large panel of human tumours available in the "Cancer Genome Atlas Research Network" (Cancer Genome Atlas Research Network *et al*., 2013; Domcke *et al*., 2013). In this study, cancer cell lines were cultured in monolayer/2D layouts. However, there are some limitations of 2D *in vitro* assays since they may not accurately reflect the complex 3D tumour environment. Cell behaviour is compromised when cells are grown in monolayer on flat dishes because this phenomenon is

highly dependent on interactions within a 3D environment. Indeed, 3D cultures offer more physiological conditions, similar to an *in vivo* situation, compared to monolayer cultures (Ravi *et al*., 2015). In our future studies, 3D culture conditions will be considered.

1.9 *In vitro* cell viability assays

Traditional methods such as counting viable cells based on trypan blue dye exclusion assay using a hemocytometer are simple but very time consuming and sometimes inaccurate (Kanemura *et al*., 2002). Now-a-days, a plethora of methods exist to assess the viability of *in vitro* cultured cells and cytotoxicity of compounds (Riss *et al*., 2013). Establishing a consistent and reproducible procedure is important. Depending on the methods of measurement these are often subdivided into four groups: clonogenic, radioactive, colorometric and fluorometric (Al-Nasiry *et al*., 2007; Vega-Avila and Pugsley, 2011). In this study, colorometric and clonogenic assays were performed.

MTS (3- (4,5-dimethylthiazol-2-yl) -5- (3-carboxymethoxyphenyl) -2- (4-sulfophenyl) - 2H-tetrazolium) assay has been used since 1991 (Cory *et al*., 1991). It avoids the error prone solubilisation step which is required in MTT (3-(4,5-dimethylthiazol-2-yl)-2,5-diphenyltetrazolium bromide) assay (Dias *et al*., 1999). MTS assay is free from serious artifacts and uniquely precise (Goodwin *et al*., 1995). Viable cells reduce MTS into a soluble perceivable hue which is measured at 390 nm wavelength. Dead cells do not have this intrinsic ability to perform this activity, hence the colored product correlates with viable cells in culture (Cory *et al*., 1991; Riss *et al*., 2013). It is therefore possible to utilize this assay to predict cytotoxicity of any compound of interest.

The clonogenic assay has been introduced for more than 50 years ago (Puck and Marcus, 1956). Clonogenic assay is the most widely used *in vitro* assay to determine the drug response to tumours that provides the medical oncologists with the necessary data to define beneficial drug regimens (Hoffman *et al*., 1991). At least in some cases clonogenic assay can partly replace animal studies for cancer drug evaluation (Hoffman *et al*., 1991). The survival of the proliferating cells is assessed by their ability to form colonies (Lu and Wong, 2005). The assay tests the ability of cells to undergo unlimited division. Cells are usually allowed to grow up to 1-

3 weeks depending on their colony forming ability. After the incubation period, colonies are fixed and stained with glutaraldehyde and crystal violet respectively (Nicolaas *et al*., 2006). However, clonogenic assay has some limitations such as the ability to measure cell death at a low range of drugs, while clinical responses require a high dose range, clump artifacts, lack of cytotoxic end-points and loss of normal cell-cell interactions etc (Weisenthal *et al*., 1985; Hoffman *et al*., 1991).

1.10 Target protein detection by Western blotting

Western blotting has been in practice since 1979 (Towbin *et al*., 1979). It is one of the most important techniques used in cell and molecular biology to identify specific proteins from a complex mixture of proteins extracted from cells. Protein is separated by size, transferred to a solid support and visualized by using a proper primary and secondary antibody (Mahmood and Yang, 2012).

One of the drawbacks of Western blotting is that the data produced are semi-quantitative. This is because, it provides a relative comparison of protein levels but not an absolute measure of quantity. The chemiluminescent signal generated during detection of proteins is not linear across the concentration range of samples (Mahmood and Yang, 2012). However, Western blot data are quantitatively interpreted in terms of fold changes in protein expression between samples (Sean *et al*., 2014). In this regard, appropriate selection of housekeeping proteins (HKPs) and total proteins are important for normalizing the data to assure that the reported fold changes of the target proteins are correct.

1.11 *In vitro* cell based imaging by fluorescence microscopy

Imaging is a valuable readouts of drug activity for *in vitro* cancer studies. Molecular imaging facilitates the assessment of the temporal and the spatial dissemination of biological processes in an intact living cell. With these approaches, more meaningful results can be achieved that are comparable with other *in vitro* methods (Weissleder, 2002). In imaging, tagged molecules can be viewed leading to insights on cell function, and the effectiveness of particular therapies (Cho *et al*., 2006; Sarker and Workman, 2007). However, a single technique alone is not sufficient to answer all the research quires. Therefore, techniques are chosen based on their feasibility. In our

study, fluorescence microscopy was used to visualize the expression of a fluorescently labeled phospho-AKT (Ser473) protein.

Fluorescence microscopes were developed at the beginning of the 20th century (Köhler, 1905). Fluorescence microscopy is now being widely used in cell biological research to study fixed and living cells because of its versatility, specificity, and high sensitivity. Usually, mercury lamps are used as a light source for excitation of fluorochromes. Protein of interest can be marked with such fluorochromes via antibody staining which allows the assessment of the distribution of that single molecule species, its amount and localization inside a cell. A bandpass filter (excitation filter) is located between the light source and the specimen which efficiently restricts the range of excitation light. The excitation light excites the molecule to a higher level of vibrational energy, introducing an excited state. After the lifetime of the fluorescence agent, excited state returns to the ground state by releasing excess energy as a light photon (fluorescence emission). An emission filter (bandpass or longpass) is placed between the detector and the specimen that blocks the excitation light and allows only the emitted light to be transmitted (Figure 7). As the emitted light has a longer wavelength than the excited, hence the emitted light can pass through the emission filter that prevents the final image from distortions. The images are often detected by a charged couple device (CCD) or a photomultiplier tube (PMT) and displayed on a computer screen (Ishikawa-Ankerhold *et al*., 2012). Hoechst-33342 is often used in live cells (Purschke *et al*., 2010) and DAPI is often used in fixed cells to analyze DNA (Chazotte *et al*., 2011). A number of fluorochromes are available to mark the target proteins for example GFP (Benchaib *et al*., 1996). Photobleaching characteristic of the fluorochromes is a major problem associated with fluorescence microscopy. Reducing excitation light and exposure time can be beneficial to minimize photobleaching (Douglas *et al*., 1985).

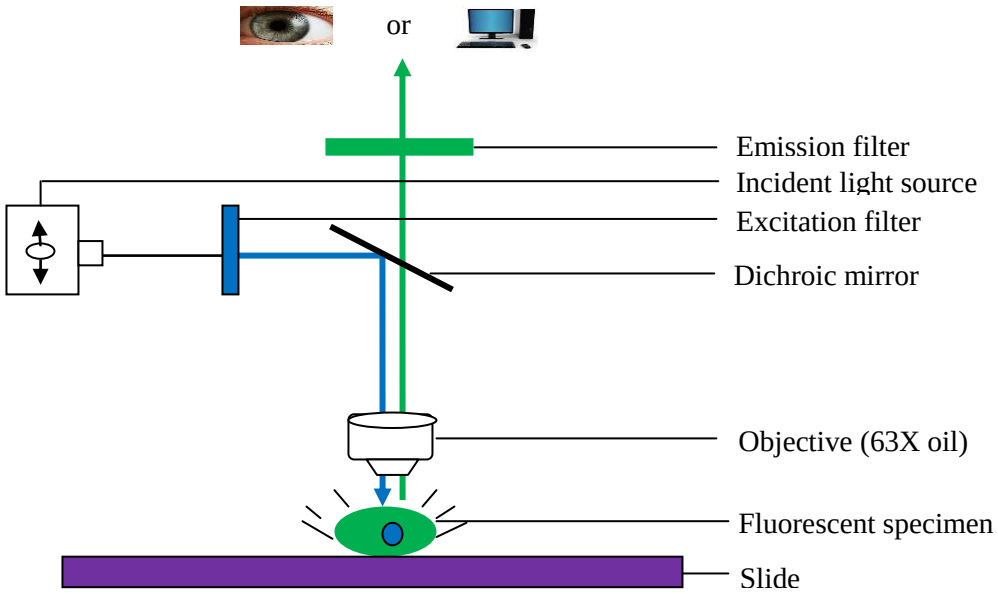

Figure 7: Principle of a fluorescence microscopy. Light of the desired excitation wavelength is focused on the specimen through the objective lens. The fluorescence emitted light is passed through the same objective to the detector (epifluorescence microscopy). A dichroic mirror allows the emitted light to pass through that prevents reflected excitation light entering the optics. Furthermore, emission filter is used to avoid the signal-to-noise ratio which only allows light of the desired emission wavelength to pass through (Modified from Webb and Brown, 2013).

Chapter 2

Aims of the Study

GBM poses a major medical challenge and the prognosis is dismal. *De novo* or acquired resistance to standard of care therapies is a major obstacle to effective treatment. As such, there is a need to develop new therapeutic agents. AKT is one of the key oncogenic kinases regulating gliomas. The main goal of the Master's project was to investigate the AKT pathway using allosteric and ATP competitive inhibitors of AKT in GBM cell lines. In particular, the following objectives have been defined within the work:

1. To investigate the therapeutic potential of AKT inhibitors in GBM cell lines with different genetic backgrounds
2. To determine the antiproliferative effects of the AKT inhibitors in GBM
3. To elucidate the cellular death mechanism induced by AKT inhibition

Chapter 3

Materials and Methods

This study was conducted from 01 August 2015 to 01 April, 2016 at the Department of Biomedicine, University of Bergen, Norway to investigate the role of allosteric and ATP competitive kinase inhibitors of AKT in human GBM cell lines.

3.1 Experimental cell lines

- SKMG-3: PTEN-null , EGFR-amplified
- U-87: PTEN-null , EGFR-low

Cell lines were provided by the Department of Biomedicine, University of Bergen.

3.2 Cell culture

3.2.1 Equipments and reagents for cell culture

- 75 cm^2 cell culture flasks (Thermo fisher scientific, USA)
- DMEM medium (D5671, Sigma-Aldrich, UK) supplemented with necessary reagents
- Trypsin EDTA (BE17-161E, Biowhittaker, Lonza, Belgium)
- PBS (D1408, Sigma-Aldrich, USA)

3.2.2 Reagents preparation for cell culture

- **1X PBS**: 1X PBS was made by diluting 50 ml of 10X PBS in 450 ml Milli-Q water.

3.2.3 Procedure of cell culture

Cells were cultured in 75 cm^2 culture flask, added with 20 ml of Dulbecco's Modified Eagle's Medium (DMEM). Media was supplemented with 50 ml of 11.11% fetal bovine serum (FBS), 10 ml of 2.2% pen-strep, 10 ml of 2.2% L-glutamine, 16 ml of 3.5% non-essential amino acid (NEAA) and 100 µl of 0.02% plasmocin into 450 ml of DMEM. When cells reached 80% of confluency medium was removed from culture flask by aspiration and washed the monolayer with 1X PBS free of Ca^{2+} and Mg^{2+} to remove all traces of serum. PBS solution was then removed by aspiration.

Sufficient volume of Trypsin/EDTA solution was dispensed into culture vessel to thoroughly cover the monolayer of cells and placed in 37°C incubator for around 3 minutes. Flasks were examined under an inverted microscope to check the detachment of cells from the surface. After trypsinization serum containing culture medium was added to the cell suspension to inhibit further trypsin activity which can damage cells. Trypsinization dissociated cells from each other and also from the surface of the culture flask. Cell suspension was gently pipetting up and down to break up the clumps. Passage number was demarcated on the flask after each passaging.

3.3 Cell lines library construction

3.3.1 Equipments for cell library construction

- Cryovials (377224, Thermo fisher scientific, Denmark)
- Centrifuge machine (5810R, Eppendorf, Germany)
- -80 freezer/nitrogen tank
- Disposable, sterile 50 ml falcon tubes
- Isopropanol box
- Automated Cell Counter (PHCC20060, Millipore, USA)

3.3.2 Reagents for cell library construction

- Freezing medium (8% DMSO, 20% fetus bovine serum, 72% DMEM medium)

3.3.3 Procedure of cell library construction

Library of cell lines was prepared considering the fact that these cells are valuable resources and their replacements are expensive and time consuming. Cells were frozen down and preserved for later use in case of any contamination or unwanted morphological changes of the running batch.

Isopropanol box was kept at room temperature. Freezing medium was stored at -20°C freezer. Freezing medium was thawed before use. Adherent cells were gently detached from the culture flask and followed the procedure used during the subculture. Cells were resuspended in DMEM medium and the total number of cells was counted using an automated cell counter and desired volume of freezing medium was calculated (50,000 cells/ml). Cell suspension was centrifuged at 600g for 5 minutes at 4°C. Supernatant was decanted inside the laminar air flow hood without

disturbing the cell pellet. Cell pellet was resuspended in cold freezing medium. Cell suspension was aliquoted into cryogenic storage vials and gently mixed the cells to maintain a homogeneous cell suspension. Cryovials containing the cells were kept in an isopropanol box and stored at -80°C overnight. Frozen cells were then stored in the gas phase above the liquid nitrogen.

3.4. Cell counting

3.4.1 Equipments for cell counting

- Automated cell counter with 60 µM sensors (PHCC20060, Millipore, USA)
- Incubator

3.4.2 Reagents for cell counting

- Trypsin EDTA
- DMEM medium supplemented with necessary reagents

3.4.3 Procedure of cell counting

Cells, about 80% of confluency were rinsed with 5 ml of 1X PBS and treated with 2 ml of trypsin EDTA. The flask was incubated for 3 minutes in the incubator (37°C and 5% CO_2). Approximately, 10 ml of DMEM was added in the culture flask, pipetted up and down gently and the suspension was taken into a falcon tube. 100 µl cell suspension was taken into an eppendorf tube for cell counting by an automated cell counter.

3.5 Cell viability assay

3.5.1 Equipments for determining cell viability assay

- 96 well plates (167008, Thermo fisher scientific, Denmark)
- Incubator (45762-2098, Forma scientific, USA)
- Spectrophotometer (3579032231, Thermo fisher scientific, China)

3.5.2 Reagents for determining cell viability assay

- **MTS** (G3580, Promega, USA)
- **AKT inhibitors** (GSK-2141795: A-1504, Active Biochem, USA; GDC-0068: A-1205, Active Biochem, USA; MK-2206: S1078, Selleckchem, Germany; GSK-690693: S113, Selleckchem, Germany)

3.5.3 Principle of cell viability assay

It is a colorimetric assay for assessing the cellular enzymatic activity. However, the exact mechanism of MTS reduction is not well understood but likely involves reaction with NADH or similar reducing molecules (O'Toole *et al*., 2003; Berridge *et al*., 2005). Tetrazolium reagent is used in combination with phenazine methyl sulfate (PMS), an intermediate electron acceptor. PMS which can enter into viable cells and transfer electrons from the cytoplasm or plasma membrane to enable the reduction of the tetrazolium into soluble formazan product. Formazan product that has an optimal absorbance at 390 nm.

3.5.4 Procedure of cell viability assay

5000 cells per 100 µl of medium were seeded in a 96 well plate and incubated overnight in an incubator. On the following day, cells were treated with increasing concentrations of drugs for 72 hours. Allosteric and ATP competitive AKT inhibitors were used as the cell growth inhibitors. DMSO, resembling the highest concentration of the drugs was used as control. After 72 hours of drug treatment, 20 µl of MTS reagent was added to each well and incubated for 4 hours. Absorbance at 390 nm wavelength was measured by spectrophotometer. IC_{50} values were calculated using GraphPad Prism-6 software. IC_{50} value is the inhibitory concentration of a drug at which 50% inhibition of the cells attained *in vitro.*

3.6 Clonogenic assay

3.6.1 Equipments for clonogenic assay

- 6 well plates (140673, Thermo fisher scientific, USA)
- Incubator

- Spectrophotometer

3.6.2 Reagents for clonogenic assay

- Crystal violet dye
- DMEM medium (10% FBS)
- 1X PBS
- 5% neutral buffered formaldehyde

3.6.3 Procedure of clonogenic assay

SKMG-3 and U-87 cells were seeded in 6 well plates (1,000 cells/well). After 24 hours, cells were treated with increasing concentrations of drugs and incubated for 11 days. Cells were grown in a humidified 5% CO_2 environment at 37°C. In between the incubation period cells were replenished once with freshly prepared drugs. DMSO was used as a control.

The procedures regarding on fixing and staining of colonies were performed in a fume hood. The media was gently removed from each of the wells by aspiration. Each well was washed with 1X PBS. Colonies were fixed with 5% neutral buffered formaldehyde solution for 15 minutes and stained with 0.01% (w/v) crystal violet in dH_2O for 30 minutes. Excess crystal violet dye was washed with dH_2O.

3.6.4 Quantification of colonies

3.6.4.1 Equipments for colony quantification

- Spectrophotometer

3.6.4.2 Reagents for colony quantification

- 10% acetic acid

3.6.4.3 Procedure of colony quantification

The crystal violet staining of cells was solubilized in 10% acetic acid. The absorbance of the solution was measured at a wavelength of 590 nm (Guzmán *et al*., 2014).

3.7 Quantification of total protein concentration

3.7.1 Equipments for quantification of total protein concentration

- 96 well plates
- Incubator
- Spectrophotometer

3.7.2 Reagents for quantification of total protein concentration

- Bicinchoninic acid **(**BCA) Reagent A (QD215382, Thermo fisher scientific, USA). BCA Reagent A contains sodium carbonate, sodium bicarbonate, pierce BCA detection reagent, and sodium tartrate in 0.1 N sodium hydroxide.
- BCA Reagent B (1859078, Thermo fisher scientific, USA). BCA Reagent B contains cupric (II) sulfate
- RIPA buffer (89900, Thermo fisher scientific, USA)

3.7.3 Reagents preparation for quantification of total protein concentration

- **Mixed BCA reagent:** 9.8 ml BCA reagent A was mixed with 200 µl BCA reagent B to make 10 ml of mixer solution.
- **RIPA buffer solution:** The solution contains 5 mM Tris HCl (pH 7.6), 150 mM NaCl, 1% NP-40, 1% sodium deoxycholate, 0.1% SDS. In addition, 1 tablet of protease inhibitor (S8820, SigmaFast™, USA) and 1 tablet of phosphatase inhibitor (04906837001, Roche, Germany) were dissolved in 10 ml of RIPA buffer.

3.7.4 Principle of BCA assay

BCA assay is a colorimetric assay. In this method, cupric ions (Cu^{2+}) are reduced to cuprous ions (Cu^{+}) by the proteins in an alkaline condition (the biuret reaction) which are then chelated by BCA. Each Cu^{+} cation is chelated by two molecules of BCA that produces a water soluble purple colored reaction product which is measured at 562 nm. The absorbance has a linear correlation with increasing protein concentrations over a broad range of 20 to 2000 µg/ml.

3.7.5 Procedure of quantification of total protein concentration

The cultured cells were harvested by the scraper and taken into the eppendorf tubes and immediately lysed by the lysis buffer. The lysed cells were sonicated (60 seconds) for disrupting the cell membrane. In a 96 well plate, 200 µl of BCA mixture solution was added in each well. Standards and samples were loaded as triplicates, 2 µl each. The plate was then incubated at 37°C for 45 minutes with gentle shaking. The absorbance was taken at 562 nm by spectrophotometer. Bovine serum albumin was used as a protein standard that was serially diluted with the blocking buffer at a 1:1 ratio (Figure 8). The standard curve analysis (Y=a+bx, Y=known absorbance, a=slope, b=y intercept and x=unknown concentration) was used to measure the total protein concentration.

3.8 Western blotting

Western blotting was performed to identify the target proteins from a complex mixture of proteins extracted from cells treated with control (DMSO), AKT inhibitors, Staurosporine (S-4400, Sigma-Aldrich, USA). The technique follows three steps: (1) gel electrophoresis to separate proteins by size (2) electrotransfer to a solid support and (3) tagging target protein with a proper primary and secondary antibody to visualize (Mahmood and Yang, 2012).

3.8.1 Gel electrophoresis

3.8.1.1 Equipments for gel electrophoresis

- Nupage™ Precast Gel (4-12%) (NP0321BOX, Thermo fisher scientific, USA)
- Gel electrophoresis cassette
- Power supply system (164-5050, PowerPac™, Bio-Red, USA)

3.8.1.2 Reagents for gel electrophoresis

- 2X Laemmli sample buffer (161-0737, Bio-Rad, USA)
- MOPS running buffer (1658658, Novex, Life technologies, USA)

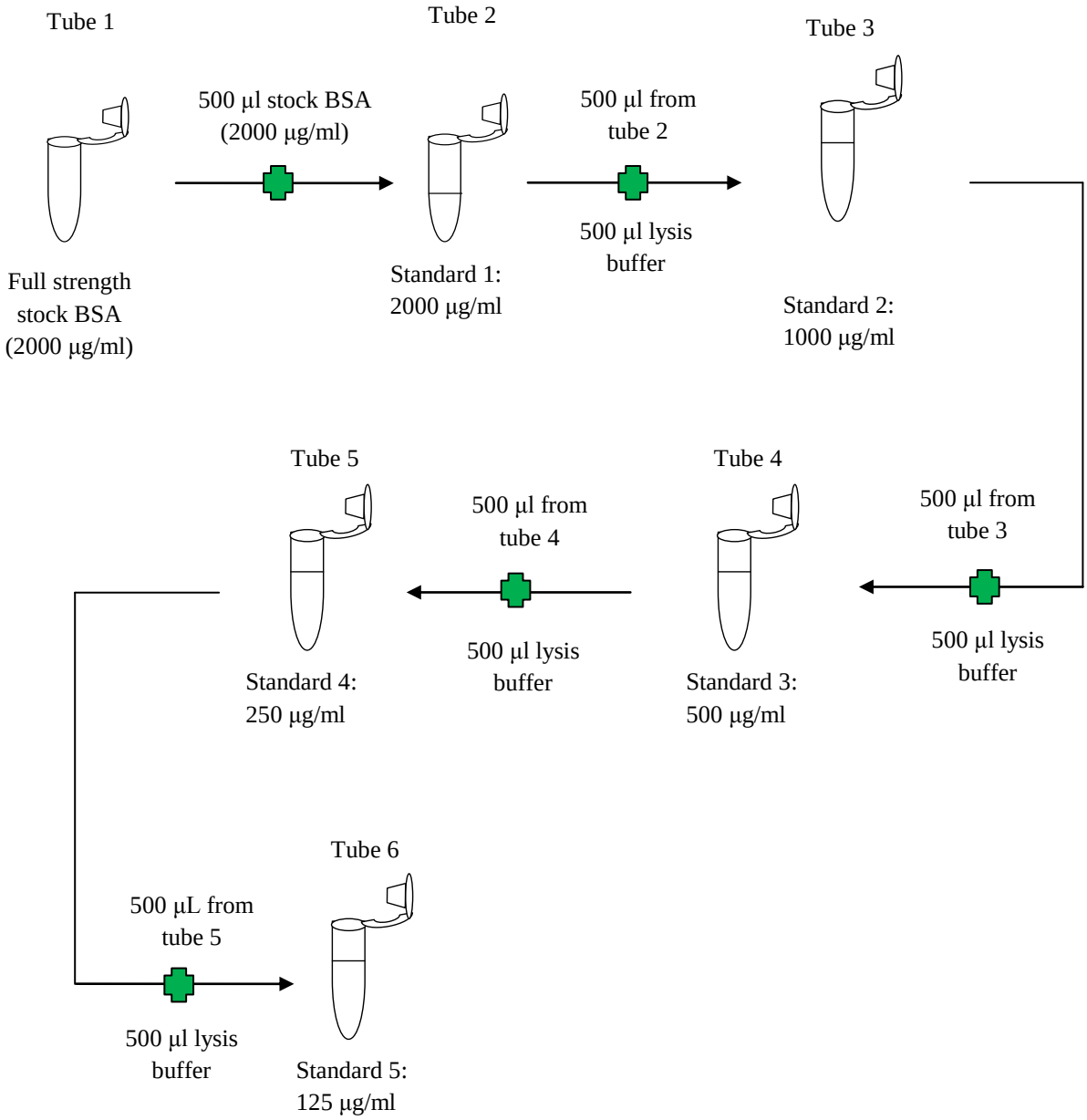

Figure 8: BSA stock solution preparation (125-2000 µg/ml). The standard, bovine serum albumin was serially diluted in the blocking buffer at a 1:1 ratio.

3.8.1.3 Reagents preparation for gel electrophoresis

- **Laemmli sample buffer:** 2X Laemmli sample buffer contains a mixture of 65.8 mM Tris-HCl (pH 6.8), 26.3% (w/v) glycerol, 2.1% SDS and 0.01% bromophenol blue. The pH of the solution is 6.8. Reducing agent, β-mercaptoethanol (10%) was added to the buffer prior to mixing with the sample. The β-mercaptoethanol facilitates proper separation of the proteins based on their size by reducing inter and intra molecular disulfide bonds of the proteins. The SDS detergent does not only denature the proteins but also binds to the positive charges of a protein. Thus giving each protein the same overall negative charge for which proteins are separated based on their size. Bromophenol blue is used as an indicator dye. Glycerol increases the density of the sample so that sample does not come out from the well.

- **MOPS running buffer (1X):** Milli-Q water, 950 ml was added into 50 ml of 20X stock solution to make 1L of 1X Running buffer. The composition of 20X MOPS stock solution is 50 mM MOPS (3-(N-morpholino) propane sulfonic acid), 50 mM Tris Base, 0.1% SDS, 1 mM EDTA. The solution has a pH of 7.7.

3.8.1.4 Sample preparation for gel electrophoresis

Sample volume that contains 20 µg of protein was taken (calculated from the standard curve analysis) in an eppendorf tube. 2X laemmli sample buffer was added as the half volume of the sample to maintain its concentration of 1X. The sample mixture was then heated at 70° for 10 minutes.

3.8.1.5 Procedure of gel electrophoresis

Precast Gel (4-12%) was used to separate the polypeptides by size. The white tape at the bottom of the gel cassette was removed and then placed in the slot of the Criterion™ tank. The chamber of the tank was blocked by a barrage and locked. The chamber was filled by around 50 ml of fresh 1X running buffer and the rest of the tank was filled by previously used running buffer (approximately 400 ml). The comb of the wells was removed carefully by pulling upward. The protein standard ladder and prepared samples were loaded in the wells of the gel using a

micropipette with gel loading tips. The lid was fit onto the tank and plugged into the power source. The electrophoresis was run for about one and half hour (150V). Electrophoresed gel was drawn from the gel cassette and the tank was rinsed with UF (Ultrafiltration) water.

3.8.2 Electrotransfer of proteins

3.8.2.1 Equipments for electrotransfer of proteins

- Plastic cassette
- Paper pad
- Gel
- Nitrocellulose membrane (G9890277, GE healthcare life sciences, Germany)
- Roller

3.8.2.2 Reagents for electrotransfer of proteins

- Transfer buffer (1676236, Novex, Life technologies, USA)

3.8.2.3 Reagents preparation for electrotransfer of proteins

- **Transfer buffer (1X):** 850 ml of Milli-Q water and 100 ml of methanol were added into 50 ml of 20X stock solution to make 1L of 1X Transfer buffer. The composition of 20X stock solution is 25 mM Bicine, 25 mM Bis-Tris (free base), 1 mM EDTA. The pH of the stock solution is 7.2.

3.8.2.4 Procedure of electrotransfer of proteins

In electrophoretic transfer, an electric field was employed to elute the proteins from electrophoresed gel and transfer them to the nitrocellulose membrane. A nitrocellulose membrane and the gel were placed together, with one filter paper and four fiber pads on top and bottom of the gel (Figure 9). Air bubbles formed between the gel and the nitrocellulose membrane were removed by gentle rolling using the roller tool. The sandwich was then placed in the blotting tank. Fresh transfer buffer was poured over the sandwich and the rest of the tank was filled with previously used transfer buffer. The lid was fit onto the tank and plugged into the power source (30 volts, 1.5 hours). After completing the run, the nitrocellulose membrane was collected carefully.

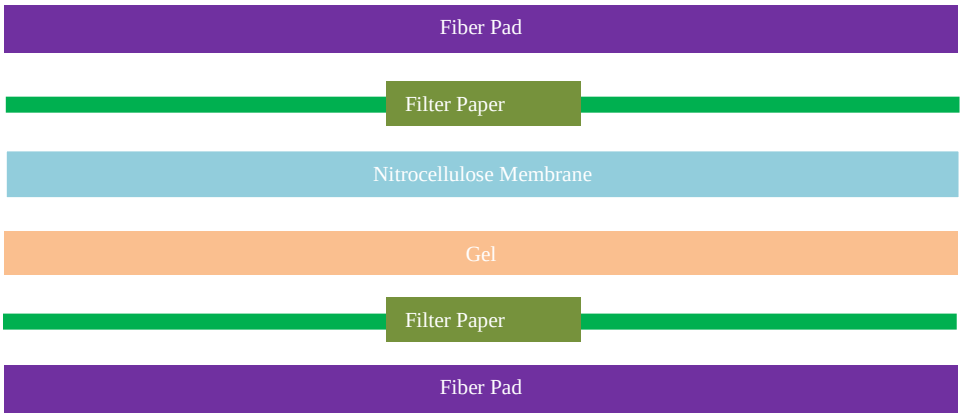

Figure 9: The orientation of a gel sandwich. Nitrocellulose membrane and gel are placed between buffer soaked filter papers. Fiber pads are placed at each end of the sandwich.

3.8.3 Blocking, antibody incubation and detection

3.8.3.1 Reagents for blocking, antibody incubation, and detection

- Phosphate buffer saline Tween (1X PBST)
- Blocking solution
- Primary antibody
- Secondary antibody (PH18900721, Thermo fisher scientific, USA)
- Enhanced chemiluminescent substrate (34095, Thermo fisher scientific, USA)
- Image Reader LAS-3000 (4622724, Fujifilm, Japan)

3.8.3.2 Reagents preparation for blocking, antibody incubation and detection

- **Phosphate buffer saline Tween (PBST):** 0.1% Tween-20 was mixed into 1X PBS.
- **Blocking solution:** 5% skim milk powder was mixed in 1X PBST. Hence 25 gm milk powder was mixed in 1X PBST.
- **Primary antibody:** Primary antibodies (Table 2) were diluted in blocking solution as 1:5000.
- **Secondary antibody:** Anti Rabbit secondary antibody was diluted as 1:10,000 in 1X PBST.

- **Enhanced chemiluminescent substrate:** Super Signal West Femto Maximum Sensitivity Substrate A (1 ml) was mixed with B (1 ml). Super Signal West Femto Maximum Sensitivity Substrate is very sensitive that can detect low femtogram amounts of protein in bands on nitrocellulose membranes.

Table 2: Primary antibodies for Western blotting

Primary antibody	Catalogue number	Supplier
Phospho-AKT (Ser473)	4058	Cell signaling technology, USA
pan AKT	4685	Cell signaling technology, USA
Phospho-PRAS40	2997	Cell signaling technology, USA
PRAS40	2691	Cell signaling technology, USA
PARP	9542	Cell signaling technology, USA
Cleaved caspase 3 (Asp175)	9661	Cell signaling technology, USA
GAPDH	ab9485	Abcam, UK

3.8.3.3 Procedure of blocking, antibody incubation and detection

The blots were incubated with specific primary and secondary antibodies respectively to visualize the desired proteins. Nitrocellulose membrane was incubated with blocking solution for an hour on a shaker to block the protein free spaces on the membrane (5% skim milk in 1X PBST). The membrane was rinsed three times in 1X PBST, 10 minutes each. The primary antibodies were diluted as 1:5000 in the blocking solution. The blots were incubated with specific primary antibodies overnight at 4°C on a shaker. On the following day, blots were rinsed three times in 1X PBST, 10 minutes each. The secondary antibody (anti rabbit) was diluted in PBST at 1:10,000 ratio. The blots were then incubated with the diluted secondary antibody for 1 hour at room temperature on an electric shaker. After that, blots were rinsed three times in PBST, 10 minutes each. Chemiluminescence detection technique, subjected to secondary antibody conjugated HRP enzyme and ECL substrate reaction, was used to detect the blotted proteins. A chemiluminescence product was formed upon addition of ECL substrate that was visualized in a digital imaging system (Image Reader LAS-3000).

3.8.4 Protein standard

The SeeBlue Plus2 Pre-Stained Standard (LC5925, Invitrogen, USA) contains a total of ten proteins. The protein mixture allows approximate calibrations of proteins in a mass range

between ~14 and 191 kDa. The standard allows quick visual assessment during electrophoresis and transfer.

3.9 Immunocytochemistry

3.9.1 Equipments for immunocytochemistry

- Fluorescence microscope (3512000236, Zeiss AXIOZ1, Germany)
- Glass cover slips (J1800AMNZ, Thermo fisher scientific, Germany)
- 24 well plates

3.9.2 Reagents for immunocytochemistry

- 4% formaldehyde
- 1X PBS
- 0.5% Triton X-100
- Primary antibody, phospho-AKT (Ser473)
- FITC conjugated anti rabbit secondary antibody (4010-02, SouthernBiotech, USA)
- Prolong Gold antifade reagent with DAPI (P36935, Molecular probes, USA)

3.9.3 Procedure of immunocytochemistry

Cells were seeded onto glass cover slips at 1000 cells/ml in 24 well plates. On the following day, cells were treated with drugs for 24 hours. Cells were then fixed with 4% formaldehyde in 1XPBS for 30 minutes at room temperature (RT). Fixed cells were washed with 1X PBS and permeabilized with 0.5% Triton X-100 in PBS for 4 minutes. After washing three times with PBS, the cover slips were incubated in blocking buffer (0.5% BSA in PBS, sterile filtered) for 15 minutes at room temperature. Cover slips were then incubated with phospho-AKT (Ser473) antibody (diluted 1:100 in blocking buffer) for 24 hours at 4°C. Wet paper towel was kept in the box to prevent the slides from drying. They were then washed twice with PBS, followed by incubation with FITC conjugated anti rabbit for 30 minutes at RT. After washing three times with PBS, the cover slips were mounted with 5 μM of Prolong Gold antifade reagent containing DAPI. Cells were examined under a Ziess fluorescence microscope with a 63X oil objective with

DAPI and FITC filter for visualizing nuclear staining and target protein coupled with FITC respectively (Figure 10). Axiovision Rel 4.8 software was used to capture the images. Two pictures of one cell (one was with DAPI and another with FITC filter) were overlaid in ImageJ software.

3.10 Statistical analysis

In this study, all the statistical analyses were performed by GraphPad Prism-6 software. The IC_{50} values of the cell viability experiment were analyzed by two tailed t-test. In clonogenic experiment, the data in figures were presented as mean ± SD (n=3).

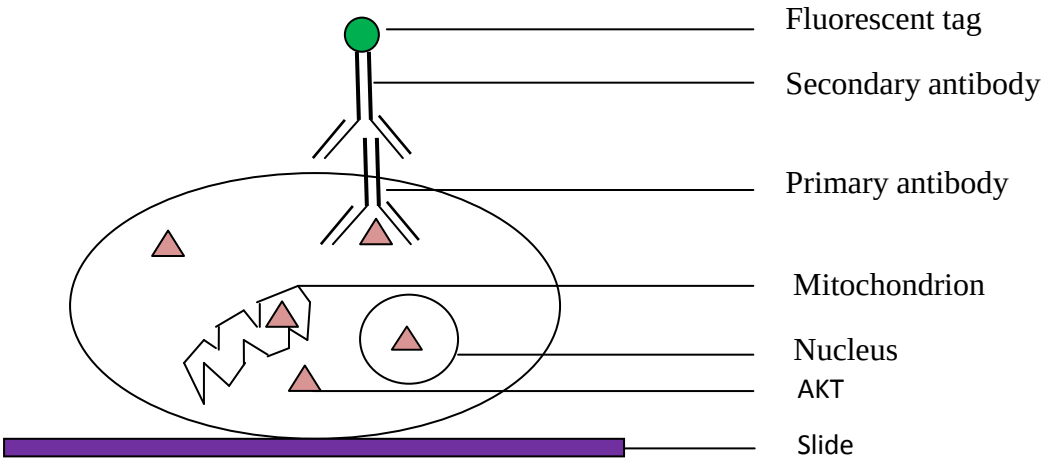

Figure 10: Immunofluorescent labeling of the target protein. Cells are fixed on the glass cover slide and then permeabilized. The epitopes of the target protein are bound with the specific primary antibody. The attached antibody is then bound with fluorescent labeled secondary antibody and visualized with the fluorescence microscope.

Chapter 4

Results

4.1 AKT inhibitors impair viability in human GBM cells

GBM cells were cultured in DMEM medium supplemented with 10% fetal bovine serum. Cells were treated with a series of concentrations of AKT inhibitors (MK-2206, GSK-2141795, GDC-0068, and GSK-690693) for 72 hours. Cell viability was measured by MTS assay. IC_{50} values were assessed using GraphPad Prism-6 software (Figure 11: A; Figure 12: A; Figure 13: A; Figure 14: A). IC_{50} value is the inhibitory concentration of a drug that determines the 50% inhibition of the cells *in vitro.*

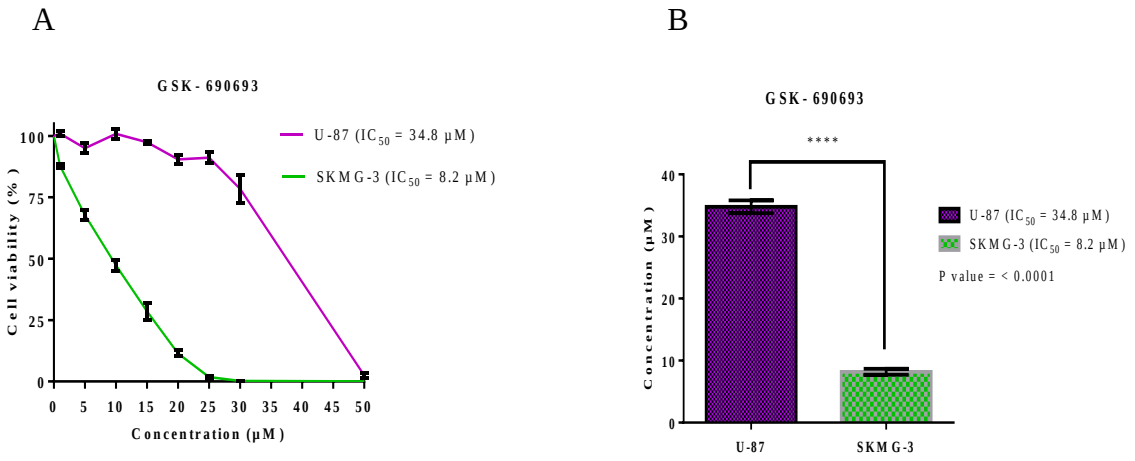

Figure 11: Effects of GSK-690693 on viability in U-87 and SKMG-3 GBM cells. (A) Viability was determined after increasing concentrations of GSK-690693. Each value (mean ± standard deviation, n= 3) of the survival rate is the percentage for the cells exposed to the drug. IC_{50} values of GSK-690693 in U-87 and SKMG-3 cells were 34.8 and 8.2 µM respectively. (B) IC_{50} values were used to test the significance of the drug response between the two cell lines. P value (<0.0001), determined from the two tailed t-test was found significant.

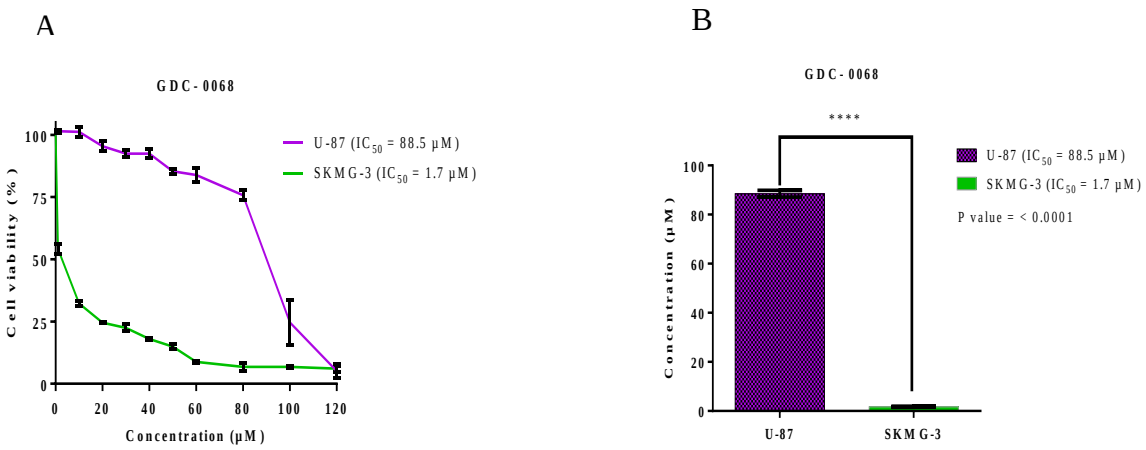

Figure 12: Effects of GDC-0068 on viability in U-87 and SKMG-3 GBM cells. (A) Viability was determined after increasing concentrations of GDC-0068. Each value (mean ± standard deviation, n= 3) of the survival rate is the percentage for the cells exposed to the drug. IC_{50} values of GDC-0068 in U-87 and SKMG-3 cells were 88.5 and 1.7 μM respectively. (B) IC_{50} values were used to test the significance of the drug response between the two cell lines. P value (<0.0001), determined from the two tailed t-test was found significant.

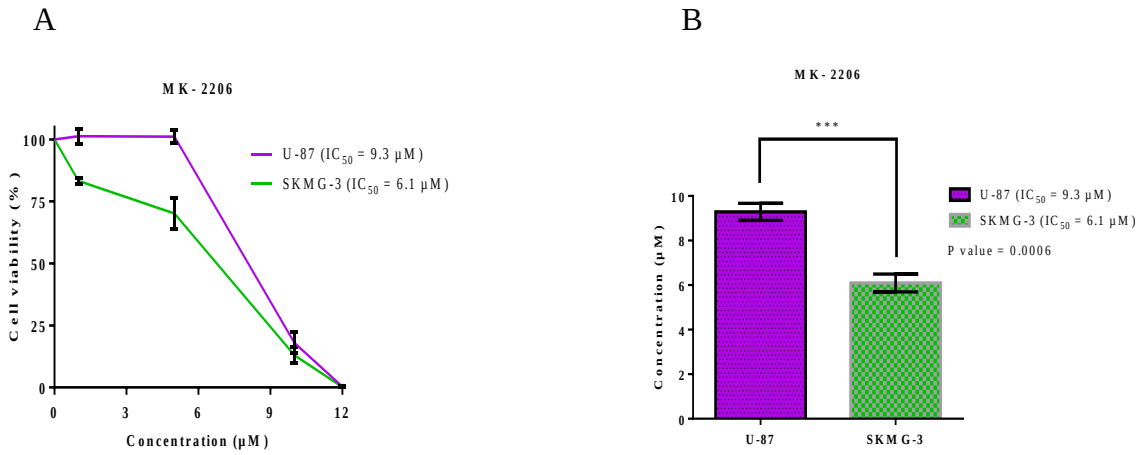

Figure 13: Effects of MK-2206 on viability in U-87 and SKMG-3 GBM cells. (A) Viability was determined after increasing concentrations of MK-2206. Each value (mean ± standard deviation, n= 3) of the survival rate is the percentage for the cells exposed to drug. IC_{50} values of MK-2206 in U-87 and SKMG-3 cells were 9.3 and 6.1 μM respectively. (B) IC_{50} values were used to test the significance of the drug response between the two cell lines. P value (= 0.0006), determined from the two tailed t-test was found significant.

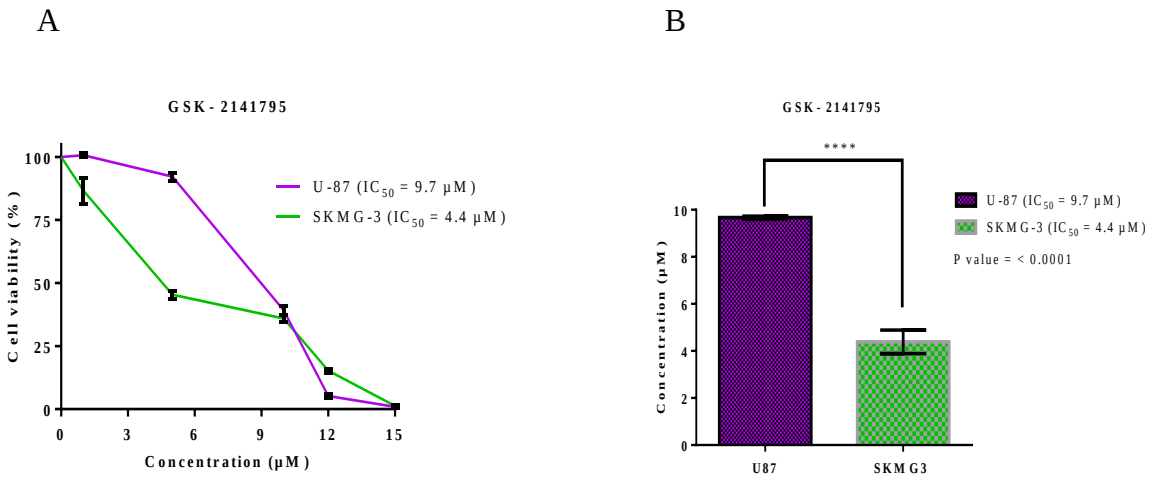

Figure 14: Effects of GSK-2141795 on viability in U-87 and SKMG-3 GBM cells. (A) Viability was determined after increasing concentrations of GSK-2141795. Each value (mean ± standard deviation, n= 3) of the survival rate is the percentage for the cells exposed to the drug. IC_{50} values of GSK-2141795 in U-87 and SKMG-3 cells were 9.7 and 4.4 μM respectively. (B) IC_{50} values were used to test the significance of the drug response between these two cell lines. P value (<0.0001), determined from the two tailed t-test was found significant.

4.2 AKT inhibitors reduce clonogenicity in GBM cells

The antiproliferative effect of the AKT inhibitors was investigated by clonogenic assay. In each well of a 6 well plate, 1000 cells were seeded. Cells were plated as triplicates. On the following day, cells were treated with MK-2206 and GSK-2141795 at concentrations of 2, 5, and 7 μM as monotherapy and DMSO as control (Figure 15: A; Figure 16: A). Cells were incubated for 11 days until colonies were clearly seen. Colonies were stained by 0.01% crystal violet dye (Franken *et al*., 2006) that primarily binds to DNA in the nucleus of mammalian cells (Gillies *et al*., 1986). Colonies were quantified by dissolving the crystal violet staining of the cells in 10% acetic acid (Kueng *et al*., 1989; Guzmán *et al*., 2014).

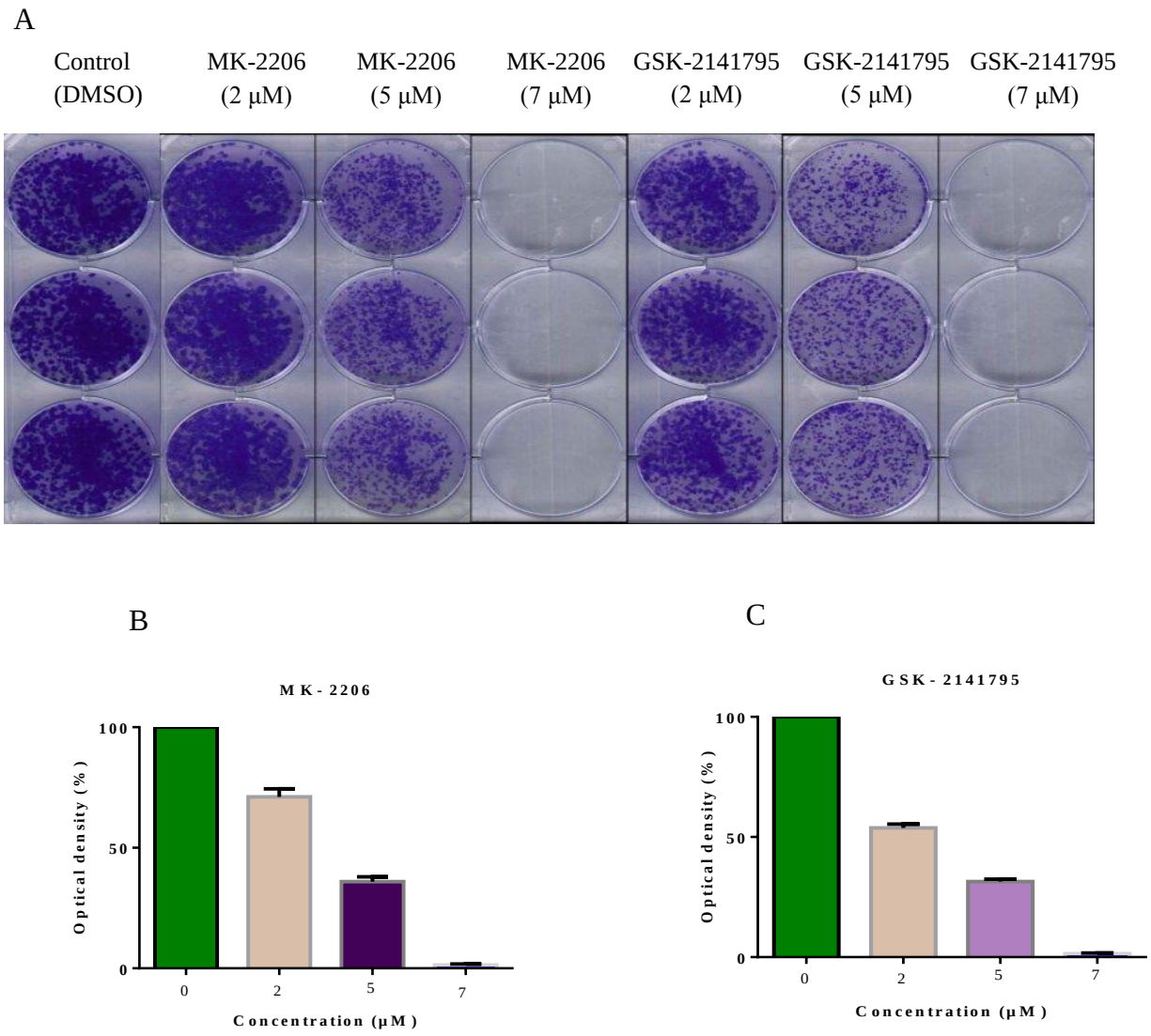

Figure 15: Effects of AKT inhibition on clonogenicity in SKMG-3 cells. (A) Representative images of the clonogenic assay of SKMG-3 cells treated with increasing concentrations of AKT inhibitors and DMSO. (B, C) Colonies were quantified by dissolving the crystal violet staining of the cells in 10% acetic acid. The absorbance of the solution was measured at a wavelength of 590 nm. The data in the graphs were presented as mean ± SD (n= 3). These are the representative results of two independent experiments.

A

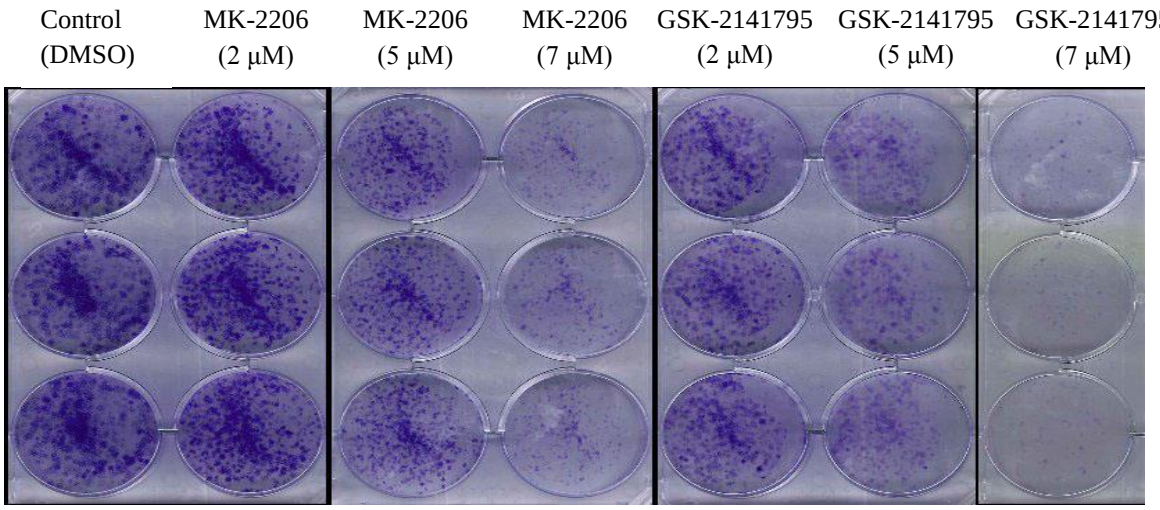

B

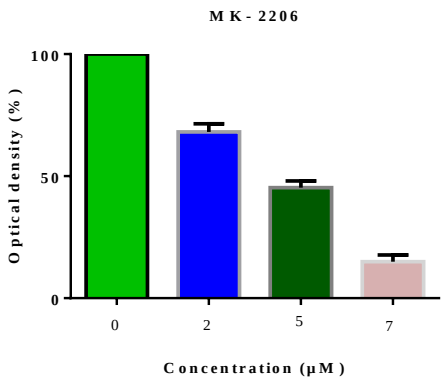

C

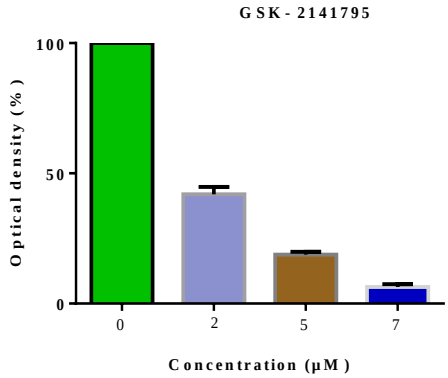

Figure 16: Effects of AKT inhibition on clonogenicity in U-87 cells. (A) Representative images of the clonogenic assay of U-87 cells treated with increasing concentrations of AKT inhibitors and DMSO. (B, C) Crystal violet staining of cells from each well was dissolved in 10% acetic acid for colony quantification. The absorbance of the solution was measured at a wavelength of 590 nm. The data in the graphs were presented as mean ± SD (n= 3). These are the representative results of two independent experiments.

4.3 AKT inhibitors affect phosphorylation of AKT and its downstream substrates

The two AKT inhibitors affected AKT-phosphorylation differently. MK-2206 decreased while GSK-2141795 increased phosphorylation of AKT (Figure 17: A; Figure 18: A). Decreased phosphorylation of PRAS40, a downstream substrate of AKT was determined (Figure 17: A, B; Figure 18: A, B). Drugs increased the levels of cleaved caspase 3, an apoptotic maker, in SKMG-3 cells (Figure 17: A) while no induction of cleaved caspase 3 was determined in U-87 cells (Figure 18: A). However, apoptosis inducing chemotherapeutic, Staurosporine showed that apoptosis pathway was prevailed in U-87 cells as determined by the increased levels of caspase 3 (Figure 19). GAPDH was used as a loading control.

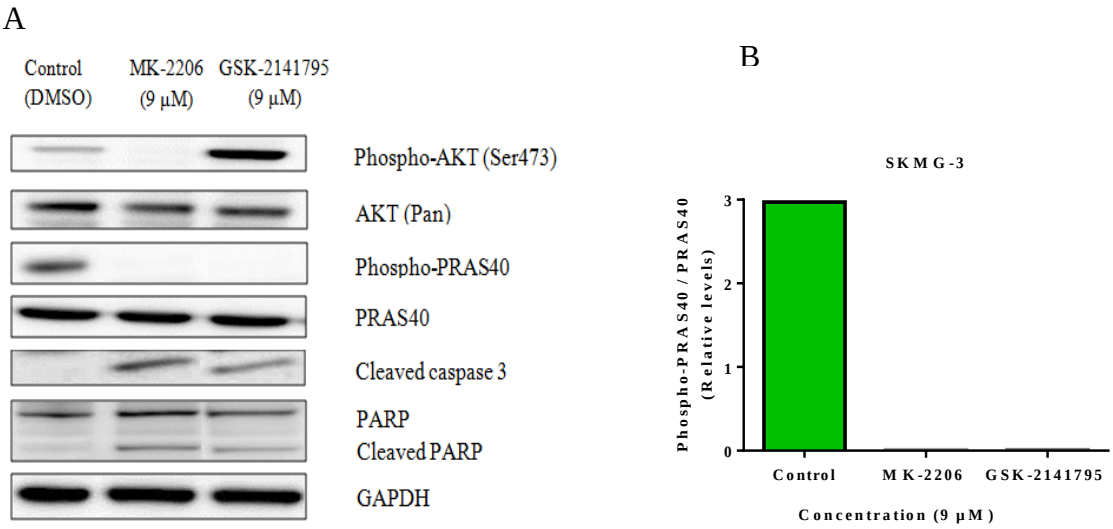

Figure 17: Assessing the effects of AKT inhibitors on downstream substrates of AKT and apoptotic markers in SKMG-3 cells. (A) Western blotting of phospho-AKT (Ser473), pan-AKT, cleaved caspase 3, phospho-PRAS40, PRAS40, PARP, and cleaved PARP was performed in protein extracts of SKMG-3 cells treated with drug control and AKT inhibitors for 24 hours at 9 µM. The blots are representative of two independent experiments. (B) Phospho-PRAS40 was normalized to its respective total protein and presented as relative fold change.

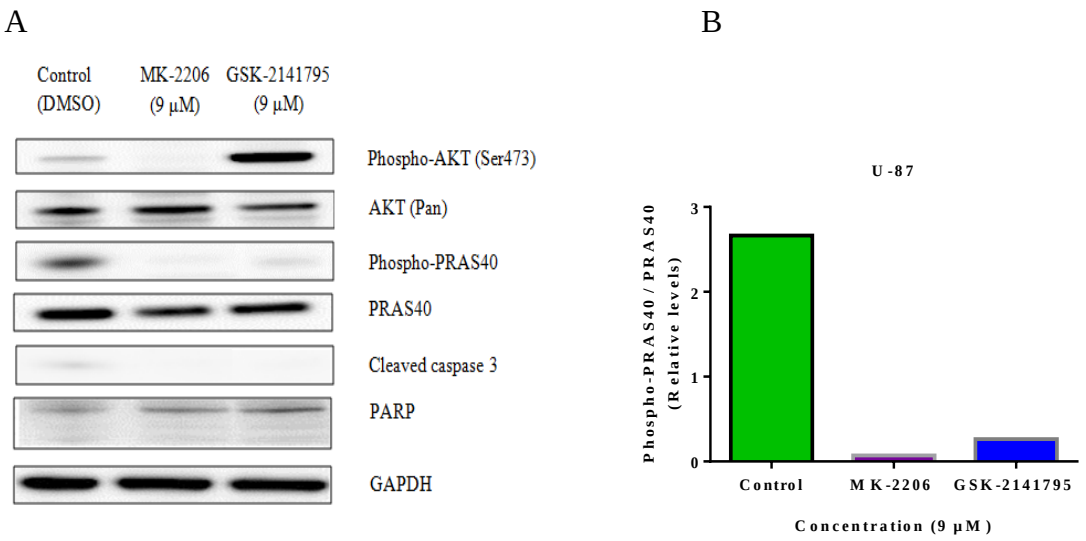

Figure 18: Assessment the effects of AKT inhibitors on downstream substrates of AKT and apoptotic markers in U-87 cells. (A) Western blotting of phospho-AKT (Ser473), pan-AKT, cleaved caspase 3, phospho-PRAS40, PRAS40, PARP, and cleaved PARP was performed in protein extracts of U-87 cells treated with drug control and AKT inhibitors for 24 hours at 9 µM. The blots are representative of two independent experiments. (B) Phospho-PRAS40 was normalized to its respective total protein and presented as relative fold change.

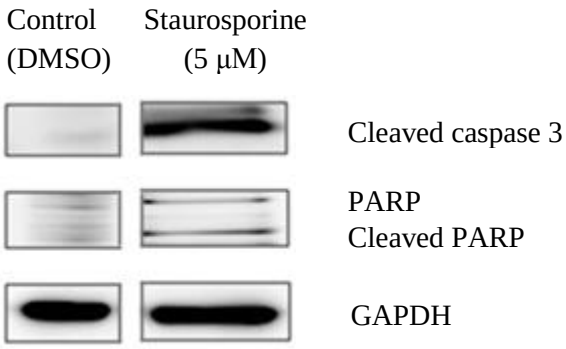

Figure 19: Staurosporine induces apoptosis in U-87 cells. Cells were incubated with 5 µM of Staurosporine and DMSO as control for 24 hours. Staurosporine increased the levels of cleaved caspase 3 which in turn generated cleaved PARP by proteolytically cleaving the total PARP.

4.4 Determining the expression of phospho-AKT by immunofluorescence

To further substantiate the Western blot data the levels of expression of phospho-AKT (Ser473) were assessed by immunofluorescence staining. It has been demonstrated that the levels of phosphorylation of AKT at 473 was reduced significantly by MK-2206 (Figure 20: B; Figure 21: B) compared to the control group (Figure 20: A; Figure 21: A). While GSK-2141795 hyperphosphorylated AKT at 473 (Figure 20: C; Figure 21: C). The levels of pan-AKT (Total AKT) were not further assessed in this study as their levels were found stable in the Western blot data.

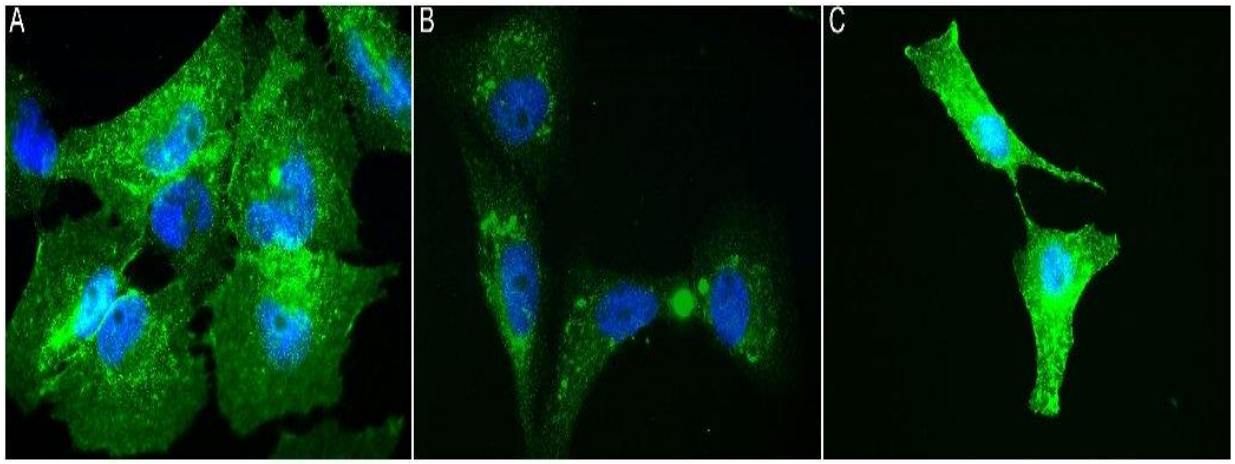

Control (DMSO) | MK-2206 (6 μM) | GSK-2141795 (6 μM)

Figure 20: Immunofluorescence staining of phospho-AKT (Ser473) in SKMG-3 cells. Expression of phospho-AKT (Ser473) in SKMG-3 cells treated with (A) DMSO, (B) MK-2206 at 6 μM, (C) GSK-2141795 at 6 μM. All the representative images were acquired after 24 hours of incubation of the cells with drugs and control. Host cell DNA was visualized with DAPI. Phospho-AKT (Ser473) was visualized with FITC fluorophore. Green and blue channels were superimposed on each other. Images were acquired with a 63X oil objective.

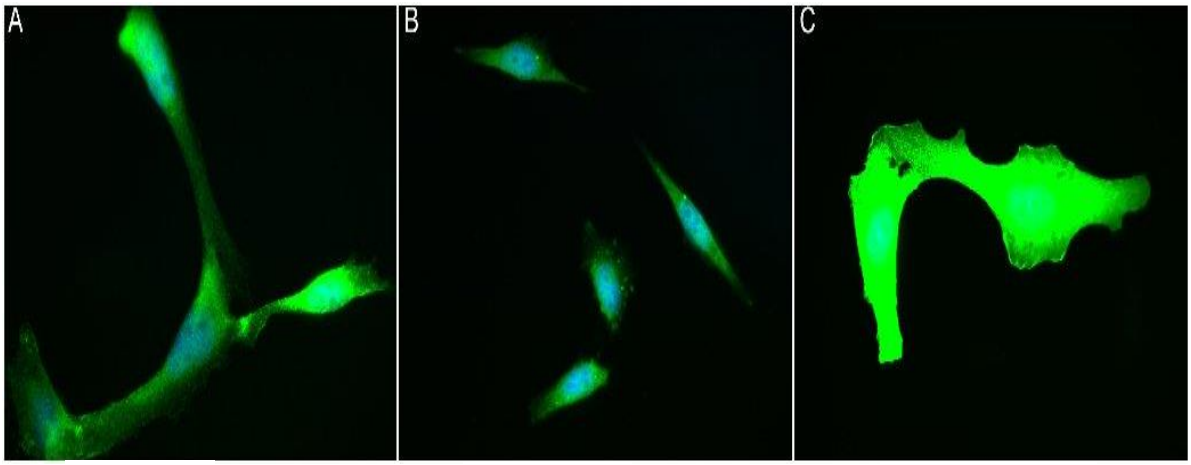

Control (DMSO)	MK-2206 (7 μM)	GSK-2141795 (7 μM)

Figure 21: Immunofluorescence staining of phospho-AKT (Ser473) in U-87 cells. Expression of phospho-AKT (Ser473) in U-87 cells treated with (A) DMSO, (B) MK-2206 at 7 μM, (C) GSK-2141795 at 7 μM. All the representative images were acquired after 24 hours of incubation of the cells with drugs and control. Host cell DNA was visualized with DAPI. Phospho-AKT (Ser473) was visualized with FITC fluorophore. Green and blue channels were superimposed on each other. Images were acquired with a 63X oil objective.

Chapter 5

Discussion

Glioblastoma is the most common primary brain tumour with a median survival of 14-15 months (Stupp *et al*., 2005). Various therapeutic approaches targeting the key molecular pathways are being studied in preclinical and clinical trials (Vacchelli *et al*., 2014). Individualized cancer therapy is no more a myth and allows for deciphering accurate individualized predictions of the likelihood of developing a disease, prognosis of the disease, and the disease susceptibility to the therapeutic agents. Each patient's genetic and clinical information are considered during this process (Van *et al*., 2010). Thus, individualized medicine helps to choose better targeted therapies and reduce healthcare costs. Although these approaches are promising, there are potential caveats to these strategies, including serious or unexpected toxic effects or the emergence of drug resistance (Shah *et al*., 2012; Lu-Emerson *et al*., 2015). Strategies involving dose escalation or combinations with other agents can be undertaken to overcome such problems.

However, data are limited in support of such an approach for GBM, and personalized medicines are not yet available in contemporary clinical neuro-oncology practice. Novel therapies targeting specific molecular pathways may offer superior efficacy and less toxicity than conventional therapies but initial clinical trials of molecularly targeted agents in brain cancer therapy are disappointing (Rich *et al*., 2004; Prados *et al*., 2006).

It has been reported that about 89.6% of tumours had at least one alteration in the PI3K pathway and 39% had two or more (Cameron *et al*., 2013). AKT is a master regulator in this pathway that has shown to promote chemo-resistance (Hafsi *et al*., 2012). Phosphorylation of AKT especially at Ser473 is associated with resistance to chemotherapy/radiotherapy (Xing *et al*., 2005; Kim *et al*., 2006; Tokunaga *et al*., 2006). Moreover, over expression of EGFR is another common aberration in primary GBM, with a frequency of 36 to 40% (Ohgaki and Kleihues, 2007). The EGFR signaling pathway further stimulates AKT activity and mediates resistance to treatment with radiation and chemotherapy (Mrinal *et al*., 2005; McDowell *et al*., 2011; Montano *et al*., 2011). In this study, the effect of AKT inhibition was investigated using allosteric and ATP

competitive kinase inhibitors in SKMG-3 (EGFR-amplified, PTEN-null) and U-87 (EGFR-low, PTEN-null) GBM cell lines.

5.1 Cellular response to AKT inhibitors

Cell viability assay was performed to assess the cytotoxic effects of the drugs. Measurement of enzymatic activity was used as a marker associated with viable cell number. Presumably, NADPH or NADH dependent dehydrogenase enzymes convert a substrate (tetrazolium) to a colored product (formazan) that is apparently directly proportional to the number of viable cells present. When cells die, they lose the ability to convert the substrate (Berridge *et al*., 2005).

In this study, one allosteric and three ATP competitive kinase inhibitors of AKT were used to assess the cellular viability of two GBM cell lines. AKT plays a key role in cell survival and proliferation. Both cell lines are PTEN-null subtypes. PTEN is a tumour suppressor that acts as a negative regulator of PI3K-AKT-mTOR signaling axis (Georgescu, 2010). In previous research it has been shown that AKT is constitutively activated in these cell lines (Daphne *et al*., 1998; Christopher *et al*., 2003). Therefore, inhibiting AKT activity by AKT inhibitors can be a potential therapeutic approach in GBM.

ATP competitive kinase inhibitors compete with ATP for occupying the ATP binding sites of AKT (Melissa *et al*., 2014). As such, inhibition of AKT activity might be delayed since some of the AKT could be occupied with ATP and become active. In this study, two ATP competitive kinase inhibitors (GSK-690693 and GDC-0068) failed to demonstrate any therapeutic efficacy in U-87 cell line and induced cell death only at a high dose above physiological range (Figure 11: A; Figure 12: A). In contrast, SKMG-3 cell line was sensitive for these drugs at <10 μM (Figure 11: A; Figure 12: A). These results demonstrate the need to identify molecular biomarkers for subgroups responding to targeted therapies.

Interestingly, another ATP competitive kinase inhibitor, GSK-2141795, exerted potent therapeutic efficacy in both cell lines. IC_{50} values of GSK-2141795 in U-87 and SKMG-3 cell lines were 9.7 and 4.4 μM respectively (Figure 14: A). The specific molecular underpinnings explaining this is unclear, but may be due to more efficient inhibition of the phosphorylation site, or from nonspecific interactions to other kinases of the AGC family (Lindsley *et al*., 2007). In

this regard, some key kinases might have been inhibited along with AKT by this inhibitor. These off targets could be assessed by mass spectrometry or protein kinase arrays (Gafken *et al*., 2006; Todd *et al*., 2013).

Recent reports have indicated that allosteric inhibitors might provide a superior efficacy over ATP competitive kinase inhibitors. The rationale for this is due to the fact that as allosteric inhibitors do not compete with ATP that render maximum inhibition of AKT by binding to the PH domain of AKT (Mohd *et al*., 2014). In this study, both of the GBM cell lines responded very well to the allosteric inhibitor. IC_{50} values of MK-2206 in U-87 and SKMG-3 cells were 9.3 and 6.1 μM respectively (Figure 13: A). This result was similar to the previous data (Figure 11: A; Figure 12: A; Figure 14: A) where it was shown that SKMG-3 cells were more sensitive than U-87 cells to AKT inhibitors. The two inhibitors (MK-2206 and GSK-2141795) that demonstrated potent physiological therapeutic efficacy in both cell lines were used for subsequent studies.

5.2 Clonogenic potential of GBM cell lines

The colony forming ability of both SKMG-3 and U-87 cells was assessed by comparing increasing concentrations of the AKT inhibitors and control (DMSO) (Figure 15; Figure 16). Usually only a fraction of the seeded cells possesses the capacity to form colonies (Haloom *et al*., 2011) and one macroscopic colony is considered to consist of at least 50 cells (Nicolaas *et al*., 2006). In this study, both SKMG-3 and U-87 cells were able to form colonies. However, U-87 cells (Figure 16: A) exhibited slower growth rate than SKMG-3 cells (Figure 15: A) as determined by their colony forming capacity in the control group. These results are supported by other reports showing that U-87 cells have a low proliferative index compared to other GBM cell lines (Xin *et al*., 2012). In both cell lines, proliferation is regulated by the PI3K-AKT pathway (Christopher *et al*., 2003; Maria *et al*., 2013). Serum factors also contribute to maintain the phosphorylation of AKT in cancer cell lines (Christopher *et al*., 2003).

Since SKMG-3 is the only glioma cell line maintaining the EGFR amplification *in vitro*, most studies on this cell line has been related to EGFR signaling and inhibition (Christopher *et al*., 2003). EGFR inhibitors such as erlotinib and gefitinib have been shown to attenuate glioma cell proliferation (Mellinghoff *et al*., 2005; Carrasco *et al*., 2011) but the results from the clinical

trials have not demonstrated any benefit on overall survival (Brandes *et al*., 2008). This is mainly attributed to intra tumoural heterogeneity of EGFR-amplified GBM cells which causes resistance to EGFR inhibitors (Alexander *et al*., 2013). Moreover, phosphatase and tensin homolog (PTEN) mutation induces hyperactivation of the PI3K/AKT pathway that renders glioma cells resistant to EGFR inhibition (Fan *et al*., 2007). A phase-I clinical trial has shown that GBM tumours that express high levels of phosphorylated AKT did not respond to erlotinib treatment (Haas-Kogan *et al*., 2005).

In this study, the antitumoural effect of MK-2206 and GSK-2141795 were assessed in U-87 and SKMG-3 cells. Both drugs impaired the colony forming ability of the cell lines in a dose dependent manner (Figure 15; Figure 16). The results suggest that AKT is a key regulator of cellular proliferation and clonogenicity. SKMG-3 cells completely lost the clonogenic potential at 7 μm concentration of both inhibitors (Figure 15), while some colonies of U-87 cells were still viable (Figure 16).

5.3 Status of downstream AKT substrates and cellular fate

In most cases, intracellular signaling cascades are regulated by either phosphorylation or dephosphorylation of signaling components (Cooper *et al*., 2000). Activation of AKT induces tumourigenicity in a variety of cancer types by phosphorylating of its downstream substrates (James *et al*., 2007). In this study, the AKT inhibitors attenuated the enzymatic activity of AKT at 9 μM, as determined by a decreased phosphorylation of PRAS40, one of the major downstream targets of AKT (Figure 17: A, B; Figure 18: A, B). PRAS40 is a raptor interacting protein that binds and inhibits mTORC1 activity (Sancak *et al*., 2007). The mechanism of action of the two different types of AKT inhibitors was different. MK-2206 led to dephosphorylation of AKT while GSK-2141795 induced hyperphosphorylation (Figure 17: A; Figure 18: A).

The inhibitors induced rapid apoptosis in SKMG-3 cells as determined by cleaved caspase 3 (Figure 17: A). Activation of caspase 3 is a hallmark of apoptosis (Shobu *et al*., 1998). All caspases are synthesized as proenzymes and activated by proteolytic cleavage (Shobu *et al*., 1998). Activated caspase 3 further cleaves several intracellular substrates (Nicholson and Thornberry, 1997). In this study, full length PARP was cleaved by the activated caspase 3

(Figure 17: A). These results were in line with previous reports describing that AKT inhibitors could induce apoptosis (Dana *et al*., 2009).

In the MTS data, it was shown that U-87 cells also died in response to the drugs treatment. Though the apoptotic pathway regulated by caspase 3 was prevailed in this cell line as determined by using Staurosporine as a positive control (Figure 19); however, apoptosis was not detectable upon AKT inhibition (Figure 18: A). Staurosporine is commonly used as a positive control for induction of apoptosis (Chafké *et al*., 2001). In future studies, autophagic markers will be investigated in this cell line because it has been reported that mTORC1, a downstream substrate of AKT, phosphorylates autophagy-related protein-13 (ATG13) and Unc-51 like autophagy activating kinase-1 (ULK1) to block the initiation of autophagy (Zoncu *et al*., 2011). As in this study, AKT activity was inhibited by AKT inhibitors which in turn possibly diminished mTORC1 activity. This diminished activity of mTORC1 could possibly induce autophagy in U-87 cells. Although autophagy is considered a protector against cell death (Mizushima, 2007), the "Nomenclature Committee" on cell death has proposed that "autophagic cell death" is another type of "active" programmed death (Galluzzi *et al*., 2012).

In both cell lines, GAPDH was assessed as a loading control to ensure equal loading of protein in each lane of the gel and for protein normalization. GAPDH is a metabolic enzyme and the levels of this protein can vary depending on the cellular context (Nicholls *et al*., 2012). However, in this study the levels of GAPDH were stable in both control and drug treated groups, hence other loading controls were not further assessed.

5.4 Immunofluorescence staining of phospho-AKT

In the present study, the phosphorylation status of AKT-Ser473 in control and drug treated groups was assessed by immunofluorescence microscopy. The allosteric drug substantially reduced phosphorylation of AKT-Ser473 in SKMG-3 (Figure 20: B) and U-87 cells (Figure 21: B) at 6 and 7 μM respectively. The ATP competitive kinase inhibitor hyperphosphorylated AKT-Ser473 in SKMG-3 (Figure 20: C) and U-87 cells (Figure 21: C) at 6 and 7 μM respectively. However, the levels of pan-AKT were not assessed. Western blot analyses showed that the levels

of pan-AKT were stable in control and drug treated groups. The primary and secondary antibody controls were not checked in this study but will be considered in future experiments.

Primary antibody control is crucial to assess the specificity of the primary antibody to the antigen. The most commonly used approach is to knock out the gene which codes the target protein. As the protein of interest is not expressed there should be no signal (Burry, 2011).

Auto-fluorescence can cause unreliable demonstration and measurement of the levels of the target protein. This is usually happened by nonspecific binding of the secondary antibody. In this regard, secondary antibody control is often used in immunofluorescence microscopy. This is performed by eliminating the primary antibody. In theory, signal should not be detected as there is no primary antibody available to bind with the secondary antibody. However, there are several potential pitfalls with this method. Nonspecific binding of the secondary antibody can result from binding to unbound aldehydes from the fixative or cell components such as histones. To solve this problem, BSA is commonly used as a blocking buffer to quench the charged sites. Moreover, the Fc region of the secondary antibody can bind to the cellular Fc receptors. This can be solved by using the Fc-end of an IgG antibody that only binds with the Fc receptors and without the propensity to bind other antigens. Normal serum from the same species is commonly used to quench Fc receptors (Burry, 2011).

In this study, two AKT inhibitors inhibited the activity of all three isoforms of AKT. As such, isoform specific phosphorylation of AKT was not investigated. In generally, AKT1 is localized to the cytoplasm, but nuclear localization is also described. AKT2 is localized to the mitochondria, while AKT3 is localized in both the nucleus and nuclear membrane (Santi and Lee, 2010). The role of AKT1 in GBM development is controversial. It has been reported that AKT1 did not seem to play a major role in GBM cell survival (Hideo *et al*., 2010). They found that AKT1 protein and mRNA levels were similar in GBM and normal control tissues. In their study, downregulation of AKT1 did not affect cell growth or survival. In contrast, in other report it has been shown that AKT1 played a critical role in the development of GBMs by up regulating the expression of cyclin D and matrix metalloproteinase-9 (MMP9) (Jian *et al*., 2011). Cell cycle progression is regulated by cyclin D which is frequently deregulated in cancer, leading to uncontrolled cell proliferation (Elizabeth *et al*., 2011). Matrix metalloproteinase-9 (MMP9) was

found to enhance invasiveness in primary GBM (Gheeyoung *et al*., 2002; Carsten *et al*., 2012). In future studies, a panel of GBM cell lines will be assessed to identify the exact role of AKT1 in GBMs. Furthermore, both AKT2 and AKT3 have been shown to stimulate GBM development and their role should be assessed in future studies (Hideo *et al*., 2010; Kristen *et al*., 2015).

Chapter 6

Conclusion

In this study, the therapeutic efficacy of AKT allosteric and ATP competitive inhibitors was investigated in EGFR-amplified SKMG-3 and EGFR-low U-87 cell lines. The IC_{50} values of AKT inhibitors were determined by cellular viability assay indicating that SKMG-3 cell line was more susceptible to AKT inhibition. These results were further validated by clonogenic assay. In clonogenic assay, both drugs completely inhibited colony forming ability of SKMG-3 cells at 7 μM dose while the effects were relatively less pronounced in U-87 cell line. Western blotting analyses demonstrated that both drugs inhibited AKT activity in both GBM subtypes as determined by dephosphorylation of PRAS40, a downstream target of AKT. Furthermore, both drugs induced rapid apoptosis in SKMG-3 cell line but failed to induce apoptosis in U-87 cell line upon AKT inhibition. In essence, EGFR-amplified SKMG-3 cells are more sensitive to AKT inhibitors than EGFR-low U-87 GBM subtype.

Chapter 7

Future Perspectives

To further substantiate the discrepant findings on apoptosis in U-87 cells, flow cytometry based on annexin-V and propidium iodide (PI) staining will be performed. In short, annexin-V and PI recognize apoptotic and necrotic cells respectively (Aja *et al*., 2011). During the early phase of apoptosis phosphatidyl serine is translocated from the inner to the outer leaflet of the plasma membrane. Phosphatidyl serine is then bound by annexin-V, labeled with a green fluorophore. However, cell membrane loses its integrity and becomes leaky in late apoptotic or necrotic events hence PI enters into cells and intercalates into nucleic acids, and displays red fluorescence (Vermes *et al*., 2000).

As EGFR-amplified GBM cells responded particularly well to AKT inhibitors, these two AKT inhibitors should be tested in primary cell lines derived from surgical specimens from GBM patients to determine whether EGFR positive tumours in general respond well to AKT targeted therapy. Furthermore, EGFR inhibitors can be tested together with AKT inhibitors as combinatorial therapy. To further elucidate this, immunodeficient mice will be implanted with tumour spheroids derived from EGFR-amplified cell lines and treated with both AKT and EGFR inhibitors. Moreover, Temozolomide, the current standard of care for GBM can be tested with AKT inhibitors for possible synergistic effects (Hegi *et al*., 2005; Kaina *et al*., 2007; Weller *et al*., 2013). The ultimate goal of this study is to identify improved therapeutic approaches for patients with GBM.

References

Aja M. R., Kimberly L. N., Jeffrey D. K., Daniel R. B. (2011) Modified Annexin-V/Propidium Iodide Apoptosis Assay For Accurate Assessment of Cell Death. *Journal of visualized experiments*, 50: 2597.

Albert J. W., Sandra H. B., Darell D. B., Kenneth W. K., Stanley R. H., Bert V. (1987) Increased expression of the epidermal growth factor receptor gene in malignant gliomas is invariably associated with gene amplification. *Proceedings of the National Academy of Sciences*, 84: 6899-6903.

Alessi D. R., James S. R., Downes C. P., Holmes A. B., Gaffney P. R. J., Reese C. B., Cohe, P. (1997) Characterization of a 3-phosphoinositide-dependent protein kinase which phosphorylates and activates protein kinase B-alpha. *Current Biology*, 7: 261-269.

Alexander S., Katrin L., Annegret K., Sabine R., Svenja Z., Adrian M., Katharina K., Manfred W., Katrin L. (2013) Erlotinib resistance in EGFR-amplified glioblastoma cells is associated with upregulation of EGFRvIII and PI3Kp110δ. *Neuro-Oncology*, 15: 1289-1301.

Al-Nasiry S., Geusens N., Hanssens M., Luyten C., Pijnenborg R. (2007) The use of Alamar Blue assay for quantitative analysis of viability, migration and invasion of choriocarcinoma cells. *Human reproduction*, 22: 1304-1309.

Andjelković M., Jakubowicz T., Cron P., Ming X. F., Han J. W., Hemmings B. A. (1996) Activation and phosphorylation of a pleckstrin homology domain containing protein kinase (RAC-PK/PKB) promoted by serum and protein phosphatase inhibitors. *Proceedings of the National Academy of Sciences*, 93: 5699–5704.

Balasis M. E., Forinash K. D., Chen Y. A., et al. (2011) Combination of Farnesyltransferase and AKT Inhibitors Is Synergistic in Breast Cancer Cells and Causes Significant Breast Tumour Regression in ErbB2 Transgenic Mice. *Clinical Cancer Research*, 17: 2852–2862.

Barnett S. F., Defeo-Jones D., Fu S., et al. (2005) Identification and characterization of pleckstrin-homology-domain-dependent and isoenzyme-specific AKT inhibitors. *Biochemical Journal*, 385: 399–408.

Barretina J., Caponigro G., Stransky N., et al. (2012) The Cancer Cell Line Encyclopedia enables predictive modelling of anticancer drug sensitivity. *Nature*, 483: 603-607.

Benchaib M., Delorme R., Pluvinage M., Bryon P. A., Souchier C. (1996) Evaluation of five green fluorescence-emitting streptavidin-conjugated fluorochromes for use in immunofluorescence microscopy. *Histochemistry and Cell Biology*, 106: 253-256.

Benedikte H., Ulrik L., Steinbjørn H., Mats H., Morten S., Michael K., Helle B., Marie-Therese S., Hans S. P. (2010) Cetuximab, bevacizumab, and irinotecan for patients with primary glioblastoma and progression after radiation therapy and Temozolomide: a phase II trial. *Neuro Oncology*: doi:10.1093/neuonc/nop063.

Berridge M. V., Herst P. M., Tan A. S. (2005) Tetrazolium dyes as tools in cell biology: New insights into their cellular reduction. *Biotechnology Annual Review*, 11: 127–152.

Brandes A. A., Franceschi E., Tosoni A., Hegi M. E., Stupp R. (2008) Epidermal growth factor receptor inhibitors in neuro-oncology: hopes and disappointments. *Clinical Cancer Research*, 14: 957-960.

Brendan D. M., Lewis C. C. (2007) AKT/PKB Signaling: Navigating Downstream. *Cell*, 129: 1261-1274.

Brognard J., Sierecki E., Gao T., Newton A. C. (2007) PHLPP and a second isoform, PHLPP2, differentially attenuate the amplitude of AKT signaling by regulating distinct AKT isoforms. *Molecular Cell*, 25: 917–931.

Brazil D. P., Yang Z. Z., Hemmings B. A. (2004) Advances in protein kinase B signaling : AKTion on multiple fronts. *Trends in Biochemical Sciences*, 29: 233–242.

Burris H. A., Siu L. L., Infante J. R., et al. (2011) Safety, pharmacokinetics (PK), pharmacodynamics (PD), and clinical activity of the oral AKT inhibitor GSK-2141795 (GSK795) in a phase I first-in-human study. *Journal of Clinical Oncology*, 29: 3003.

Burry R. W. (2011) Controls for Immunocytochemistry: An Update. *Journal of Histochemistry and Cytochemistry*, 59: 6-12.

Calleja V., Laguerre M., Parker P. J., Larijani B. (2009) Role of a novel PH-kinase domain interface in PKB/AKT regulation: structural mechanism for allosteric inhibition. *PLoS Biology*, 7: e17.

Cancer Genome Atlas Research Network, Weinstein J. N., Collisson E. A., et al. (2013) The Cancer Genome Atlas Pan-Cancer analysis project. *Nature Genetics*, 45: 1113–1120.

Carnero A. (2010) The PKB/AKT pathway in cancer. *Current Pharmaceutical Design*, 16: 34–44.

Cameron W., Brennan R.G.W., Verhaak A. M., et al. (2013) The Somatic Genomic Landscape of Glioblastoma. *Cell*, 155: 462–477.

Carrasco-Garcia E., Saceda M., Grasso S., Rocamora-Reverte L., Conde M. (2011) Small tyrosine kinase inhibitors interrupt EGFR signaling by interacting with erbB3 and erbB4 in glioblastoma cell lines. *Experimental Cell Research*, 317: 1476-1489.

Carsten H., Jelena A., Ralf-Ingo E., Giles H. V. (2012) A complete compilation of matrix metalloproteinase expression in human malignant gliomas. *World Journal of Clinical Oncology*, 3: 67–79.

Chafké A. B., Josette H., Evelyne S. (2001) Staurosporine induces apoptosis through both caspase-dependent and caspase-independent mechanisms. *Oncogene*, 20: 3354-3362.

Chazotte B. (2011) Mounting live cells onto microscope slides. *Cold Spring Harbor Protocols*, doi:10.1101/pdb.prot5556.

Cheng Y., Zhang Y., Zhang L., et al. (2012) MK-2206, a novel allosteric inhibitor of AKT, synergizes with gefitinib against malignant glioma via modulating both autophagy and apoptosis. *Molecular Cancer Therapeutics*, 11: 154–164.

Chien A. J., Cockerill A., Fancourt C., et al. (2016) A phase 1b study of the Akt-inhibitor MK-2206 in combination with weekly paclitaxel and trastuzumab in patients with advanced HER2-amplified solid tumour malignancies. *Breast Cancer Research and Treatment*, 155: 521-530.

Cho C. R., Labow M., Reinhardt M., Van O. J., Peitsch M. C. (2006) The application of systems biology to drug discovery. *Current Opinion in Chemical Biology*, 10: 294-302.

Christopher Y. T., Michael C., Michael C., Sarah P., Melody S., Roy G., Richard J., Robert W. (2003) Spontaneous activation and signaling by over expressed epidermal growth factor receptors in glioblastoma cells. *International Journal of Cancer*, 104: 19–27.

Cooper G. M. (2000) *Pathways of Intracellular Signal Transduction*. The Cell: A Molecular Approach. 2nd edition. Sunderland (MA): Sinauer Associates.

Cory A. H., Owen T. C., Barltrop J. A., Cory J. G. (1991) Use of an aqueous soluble tetrazolium/formazan assay for cell growth assays in culture. *Cancer communications*, 3: 207-212.

Daphne H., Noga S., Michelle W., Gordon M., Garret Y., David S. (1998) Protein kinase B (PKB/AKT) activity is elevated in glioblastoma cells due to mutation of the tumour suppressor *PTEN/MMAC*. *Current Biology*, 8: 1195–1198.

Dana S. L., Jason A. K., Rakesh K. (2009) AKT inhibitor, GSK-690693, induces growth inhibition and apoptosis in acute lymphoblastic leukemia cell lines. *Blood*, 113: 1723-1729.

Deborah A. A., Lili Z., Jing D., Antonio D. C., Andres J. K., Rakesh K., Joseph R. T. (2010) GSK-690693 Delays Tumour Onset and Progression in Genetically-Defined Mouse Models Expressing Activated AKT. *Clinical Cancer Research*, 16: 486–496.

Dias N., Nicolau A., Carvalho G.S., Mota M., Lima, N. (1999) Miniaturization and application of the MTT assay to evaluate metabolic activity of protozoa in the presence of toxicants. *Journal of Basic Microbiology*, 39: 103–108.

Dirk A. H., Nelson R., Jack D. L., et al. (2008) Identification of 4-(2-(4-Amino-1,2,5-oxadiazol-3-yl)-1-ethyl-7-{[(3*S*)-3-piperidinylmethyl]oxy}- 1*H*-imidazo[4,5-*c*]pyridin-4-yl)-2-methyl-3-butyn-2-ol (GSK-690693), a Novel Inhibitor of AKT Kinase. *Journal of Medicinal Chemistry*, 51: 5663–5679.

Dohrmann D., Farwell R. J., Flannery J. T. (1976) Glioblastoma multiforme in children. *Journal of Neurosurgery*, 44: 442-448.

Domcke S., Sinha R., Levine D. A., Sander C., Schultz N. (2013) Evaluating cell lines as tumour models by comparison of genomic profiles. *Nature Communications*, 4: 2126.

Douglas M., B., Joseph B., Anne L. P., Antonio M. G. J. R., Louis C. S. (1985) Digital Imaging Fluorescence Microscopy: Spatial Heterogeneity of Photobleaching Rate Constants in Individual Cells. *The Journal of Cell Biology*, 100: 1309-132.

Dumble M., Crouthamel M. C., Zhang S. Y., et al. (2014) Discovery of Novel AKT Inhibitors with Enhanced Anti-Tumour Effects in Combination with the MEK Inhibitor. *PLoS ONE*, 9: e100880.

Dunn G. P., Rinne M. L., Wykosky J., et al. (2012) Emerging insights into the molecular and cellular basis of glioblastoma. *Genes and Development*, 26: 756-784.

Eefje M. S., Lies B., Tjeerd J. P., Roeline W. P. H., Jan J. H., Martin K., Jaap C. R., Martin J. B. T. (2010) Symptoms and problems in the end-of-life phase of high-grade glioma patients. *Neuro-Oncology*: doi: 10.1093/neuonc/nop045.

Elizabeth A. M., Caldon C. E., Jane B., Andrew S., Robert L. S. (2011) Cyclin D as a therapeutic target in cancer. *Nature Reviews Cancer*, 11: 558-572.

Fan Q. W., Cheng C. K., Nicolaides T. P., Hackett C. S., Knight Z. A., Shokat K. M., Weiss W. A. (2007) A dual phosphoinositide-3-kinase alpha/mTOR inhibitor cooperates with blockade of epidermal growth factor receptor in PTEN-mutant glioma. *Cancer Research*, 67: 7960-7965.

Feng J., Park J., Cron P., Hess D., Hemmings B. A. (2004) Identification of a PKB/AKT hydrophobic motif Ser-473 kinase as DNA-dependent protein kinase. *Journal of Biological Chemistry*, 279: 41189-41196.

Franken N.A., Rodermond H. M., Stap J., Haveman J., Van B. C. (2006) Clonogenic assay of cells in vitro. *Nature Protocols*, 1: 2315–2319.

Gafken P. R., Lampe P. D. (2006) Methodologies for characterizing phosphoproteins by mass spectrometry. *Cell Communication and Adhesion*, 13: 249-262.

Galluzzi L., Vitale I., Abrams J. M., et al. (2012) Molecular definitions of cell death subroutines: recommendations of the Nomenclature Committee on Cell Death. *Cell Death and Differentiation*, 19: 107–120.

Gazdar A. F., Girard L., Lockwood W. W., Lam W. L., Minna J. D. (2010) Lung cancer cell lines as tools for biomedical discovery and research. *Journal of the National Cancer Institute*, 102: 1310-1321.

Georgescu M. M. (2010) PTEN Tumour Suppressor Network in PI3K-Akt Pathway Control. *Genes and Cancer*, 1: 1170-1177.

Gheeyoung C., Jun K. P., Lisa J., Thomas J. K., Linda M. L., Harry V. V., Timothy F. C., Paul S. M. (2002) Active matrix metalloproteinase 9 expression is associated with primary glioblastoma subtype. *Clinical Cancer Research*, 8: 2894.

Gillies R. J., Didier N., Denton M. (1986) Determination of Cell Number in Monolayer-Cultures. *Analytical Biochemistry*, 159: 109–113.

Goodwin C. J., Holt S. J., Downes S., Marshall N. J. (1995) Microculture tetrazolium assays: a comparison between two new tetrazolium salts, XTT and MTS. *Journal of Immunological Methods*, 179: 95-103.

Guzmán C., Bagga M., Kaur A., Westermarck J., Abankwa D. (2014) ColonyArea: An ImageJ Plugin to Automatically Quantify Colony Formation in Clonogenic Assays. *PLoS ONE* 9: e92444.

Haas-Kogan D. A., Prados M. D., Tihan T., Eberhard D. A., Jelluma N., Arvold N. D., Baumber R., Lamborn K. R., Kapadia A., Malec M., Berger M. S., Stokoe D. (2005) Epidermal growth factor receptor, protein kinase B/AKT, and glioma response to erlotinib. *Journal of the National Cancer Institute*, 97: 880-887.

Hafsi S., Pezzino F. M., Candido S., Ligresti G., Spandidos D. A., Soua Z., McCubrey J. A., Travali S., Libra M. (2012) Gene alterations in the PI3K/PTEN/AKT pathway as a mechanism of drug-resistance (review). *International Journal of Oncology*, 40: 639-644.

Haloom R., Christian O., George T. G., Katherine V., Assam E., Tom C. K. (2011) Clonogenic Assay: Adherent Cells. *Journal of visualized experiments*, 49: 2573.

Hanks S. K., Hunter T. (1995) Protein kinases 6. The eukaryotic protein kinase superfamily: kinase (catalytic) domain structure and classification. *The Federation of American Societies for Experimental Biology*, 9: 576–596.

Hegi M. E., Diserens A. C., Gorlia T., et al. (2005) MGMT gene silencing and benefit from Temozolomide in glioblastoma. *New England Journal of Medicine*, 352: 997-1003.

Hideo M., Kazuhito M., Keiko T. K., Yoshifumi M., Kazuyuki K., Teruyoshi K., Shinji N. (2010) AKT2 and AKT3 play a pivotal role in malignant gliomas. *Neuro-Oncology*, 12: 221–232.

Hirai H., Sootome H., Nakatsuru Y., et al. (2010) MK-2206, an allosteric AKT inhibitor, enhances antitumour efficacy by standard chemotherapeutic agents or molecular targeted drugs in vitro and in vivo. *Molecular Cancer Therapeutics*, 9: 1956–1967.

Hoffman R. M. (1991) In vitro sensitivity as a review, says in cancer: analysis, and prognosis. *Journal of Clinical Laboratory Analysis*, 5: 133-143.

Holland E. C. (2000) Glioblastoma multiforme: The terminator. *Proceedings of the National Academy of Sciences*, 97: 6242-6244.

Iacob G., Dinca E. B. (2009) Current data and strategy in glioblastoma multiforme. *Journal of Medicine and Life*, 2: 386-393.

Ishikawa-Ankerhold H. C., Ankerhold R., Drummen G. P. (2012) Advanced fluorescence microscopy techniques-FRAP, FLIP, FLAP, FRET and FLIM. *Molecules*, 17: 4047-4132.

James A. C., Vernon E. S., and Judith R. F. (2007) Targeting the AKT protein kinase for cancer chemoprevention. *Molecular Cancer Therapeutics*, 6: 2139.

James F. B., Rui X., Josef R. B., et al. (2012) Discovery and preclinical pharmacology of a selective ATP-competitive Akt inhibitor (GDC-0068) for the treatment of human tumours. *Journal of Medicinal Chemistry*, 55: 8110–8127.

Janice M. N., Suzanne J. B., Antonette C. P., et al. (1989) Mutations in the *p53* gene occur in diverse human tumour types. *Nature*, 342: 705 – 708.

Jeffrey A. U., James E. F. J (2007) Mechanisms of specificity in protein phosphorylation. *Nature Reviews Molecular Cell Biology*, 8: 530-541.

Jian Z., Kun W., Lei H., An-ling Z., Zhen-dong S., Pei-yu P., Chun-sheng K. (2011) AKT1 and AKT2 Promote Malignant Transformation in Human Brain Glioma LN229 Cells. *Journal of Cancer Research and Clinical Oncology*, 8: 144–148.

Kaina B., Christmann M., Naumann S., Roos W. P. (2007) MGMT: key node in the battle against genotoxicity, carcinogenicity and apoptosis induced by alkylating agents. *DNA Repair (Amst)*, 6: 1079-1099.

Kanemura Y., Mori H., Kobayashi S., et al. (2002) Evaluation of in vitro proliferative activity of human fetal neural stem/progenitor cells using indirect measurements of viable cells based on cellular metabolic activity. *Journal of Neuroscience Research*, 69: 869–879.

Kannan N., Haste N., Taylor S. S., Neuwald A. F. (2007) The hallmark of AGC kinase functional divergence is its C-terminal tail, a cis-acting regulatory module. *Proceedings of the National Academy of Sciences*, 104: 1272–1277.

Kim T. J., Lee J. W., Song S. Y., et al. (2006) Increased expression of phospho-AKT is associated with radiation resistance in cervical cancer. *British Journal of Cancer*, 94: 1678–1682.

Kim S., Tan A. R., Im S., Villanueva R., Valero V., Saura C., Oliveira M., Isakoff S. J., Singel S. M., Dent R. A. (2015) LOTUS: A randomized, phase II, multicenter, placebo-controlled study of ipatasertib (Ipat, GDC-0068), an inhibitor of Akt, in combination with paclitaxel (Pac) as front-line treatment for patients (pts) with metastatic triple-negative breast cancer (TNBC). *ASCO Annual Meeting*, Abstract number: TPS1111.

Knowles J. A., Golden B., Yan L., Carroll W. R., Helman E. E., Rosenthal E. L. (2011) Disruption of the AKT pathway inhibits metastasis in an orthotopic model of head and neck squamous cell carcinoma. *Laryngoscope*, 121: 2359–2365.

Köhler A., Rohr M. J. (1905) Photomicrography with ultra-violet light. *Journal of the Royal Microscopical Society*, 25: 513.

Kreisl T. N., Kim L., Moore K., Duic P., Royce C., Stroud I., Garren N., Mackey M., Butman J. A., Camphausen K., Park J., Albert P. S., Fine H. A. (2009) Phase II trial of single-agent bevacizumab followed by bevacizumab plus irinotecan at tumour progression in recurrent glioblastoma. *Journal of Clinical Oncology*, 27: 740-745.

Kristen M. T., Youting S., Ping J., Kirsi J. G., Brady B., Limei H., David E. C., Xinhui Z., Olli Y., Matti N., Ilya S., Yung W. K. A., Gregory N. F., Wei Z. (2015) Genomically amplified AKT3 activates DNA repair pathway and promotes glioma progression. *Proceedings of the National Academy of Sciences*, 112: 3421–3426.

Kueng W., Silber E., Eppenberger U. (1989) Quantification of cells cultured on 96-well plates. *Analytical Biochemistry*, 182: 16–19.

Kui L. L., Wen-I W., Joshua B., Brian B. L., Susan L. G., Guy P. A. V., Tony H. et al. (2012) An ATP-Site On-Off Switch That Restricts Phosphatase Accessibility of AKT. *Science Signaling*, 5: 2002618.

Kunihiko W., Osamu T., Kazufumi S., Yasuhiro Y., Paul K., Hiroko O. (2008) Overexpression of the EGF Receptor and *p53* Mutations are Mutually Exclusive in the Evolution of Primary and Secondary Glioblastomas. *Brain Pathology*, 6: 217-223.

Li J., Yen C., Liaw D., et al. (1997) PTEN, a putative protein tyrosine phosphatase gene mutated in human brain, breast, and prostate cancer. *Science*, 275: 1943-1947.

Lim D. A., Cha S., Mayo M. C., et al. (2007) Relationship of glioblastoma multiforme to neural stem cell regions predicts invasive and multifocal tumour phenotype. *Neuro-Oncology*, 9: 424-429.

Lin J., Sampath D., Nannini M. A., Lee B. B, Degtyarev M., Oeh J., Savage H., Guan Z., et al. (2013) *Clinical Cancer Research*, 19: 1760–1772.

Lindsley C. W., Barnett S. F., Yaroschak M., Bilodeau M. T., Layton M. E. (2007) Recent progress in the development of ATP-competitive and allosteric AKT kinase inhibitors. *Current Topics in Medicinal Chemistry*, 7: 1349-1363.

Liu R., Liu D., Trink E., Bojdani E., Ning G., Xing M. (2011) The AKT-specific inhibitor MK-2206 selectively inhibits thyroid cancer cells harboring mutations that can activate the PI3K/AKT pathway. *Journal of Clinical Endocrinology and Metabolism*, 96: 577–585.

Louis D. N., Ohgaki H., Wiestler O. D., et al. (2007) The 2007 WHO Classification of Tumours of the Central Nervous System. *Acta Neuropathologica*, 114: 97-109.

Lu-Emerson C., Duda D. G., Emblem K. E., et al. (2015) Lessons From Anti–Vascular Endothelial Growth Factor and Anti–Vascular Endothelial Growth Factor Receptor Trials in Patients With Glioblastoma. *Journal of Clinical Oncology*, 33: 1197-1213.

Lu F., Wong C. S. (2005) A clonogenic survival assay of neural stem cells in rat spinal cord after exposure to ionizing radiation. *Radiation Research*, 163: 63-71.

Ma B. B. Y., Lui V. W. Y., Hui C. W. C., et al. (2013) Preclinical evaluation of the AKT inhibitor MK-2206 in nasopharyngeal carcinoma cell lines. *Investigational New Drugs*, 31: 567–575.

Mahmood T., Yang P. C. (2012) Western Blot: Technique, Theory, and Trouble Shooting. *North American Journal of Medical Sciences*, 4: 429-434.

Maria L. C., Ana-Maria E., Adrian C. P., Radu A., Monica N., Cristiana P. T., Stefan N. C. (2013) Signal transduction molecule patterns indicating potential glioblastoma therapy approaches. *Onco Targets and Therapy*, 6: 1737–1749.

McDowell K. A., Riggins G. J., Gallia G. L. (2011) Targeting the AKT pathway in glioblastoma. *Current Pharmaceutical Design*, 17: 2411-2420.

Melissa D., Ming-Chih C., Shu-Yun Z., Michael S., Dana L., Kimberly R., Qi L., et al. (2014) Discovery of Novel AKT Inhibitors with Enhanced Anti-Tumour Effects in Combination with the MEK Inhibitor. *PLoS One*, 9: e100880.

Mellinghoff I. K., Wang M. Y., Vivanco I., Haas-Kogan D. A., Zhu S. (2005) Molecular determinants of the response of glioblastomas to EGFR kinase inhibitors. *New England Journal of Medicine*, 353: 2012-2024.

Meng J., Dai B., Fang B., Bekele B. N., Bornmann W. G., Sun D., et al. (2010) Combination treatment with MEK and AKT inhibitors is more effective than each drug alone in human non-small cell lung cancer in vitro and in vivo. *PLoS One*, 5: e14124.

Miller C. R., Perry A. (*2007*) Glioblastoma. *Archives of Pathology and Laboratory Medicine*. 131: 397-406.

Mizoguchi M., Nutt C. L., Mohapatra G., Louis D. N. (2004) Genetic alterations of phosphoinositide 3-kinase subunit genes in human glioblastomas. *Brain Pathology*, 14: 372-377.

Mizushima N (2007). Autophagy: process and function. *Genes and Development*, 21: 2861-2873.

Mohd R., Mohd A. B., Shadma P., Ghazi A. D., Galila F., Zaher. (2014) Computational Insights into the Inhibitory Mechanism of Human AKT1 by an Orally Active Inhibitor, MK-2206. *PLoS One*, 9: e109705.

Moller S., Grunnet K., Hansen S., Schultz H., Holmberg M., Sorensen M., Poulsen H. S., Lassen U. (2012) A phase II trial with bevacizumab and irinotecan for patients with primary brain tumours and progression after standard therapy. *Acta Oncologica,* 51: 797-804.

Montano N., Cenci T., Martini M., et al. (2011) Expression of EGFRvIII in Glioblastoma: Prognostic Significance Revisited. *Neoplasia*, 13: 1113-1121.

Mrinal K. G., Pankaj S., Phyllis C. H., Shaik O. R., Haque S. J. (2005) PI3K-AKT pathway negatively controls EGFR-dependent DNA-binding activity of Stat3 in glioblastoma multiforme cells. *Oncogene*, 24: 7290–7300.

Nicholson D. W., Thornberry N. A. (1997) Caspases: killer proteases. *Trends* in *Biochemical* Sciences, 22: 299–306.

Nicholls C., Li H., Liu J. P. (2012) GAPDH: a common enzyme with uncommon functions. *Clinical and Experimental Pharmacology* and *Physiology*, 39: 674-679.

Nicolaas A. P. F., Hans M. R., Jan S., Jaap H., Chris V. B. (2006) Clonogenic assay of cells in vitro. *Nature Protocols*, 1: 2315 - 2319.

Oberndorfer S., Lindeck-Pozza E., Lahrmann H., Struhal W., Hitzenberger P., Grisold W. (2008) The end-of-life hospital setting in patients with glioblastoma. *Journal of Palliative Medicine*, 11: 26-30.

Ohgaki H., Kleihues P. (2005) Epidemiology and etiology of gliomas. *Acta Neuropathologica*, 109: 93–108.

Ohgaki H., Kleihues P. (2005) Population-based studies on incidence, survival rates, and genetic alterations in astrocytic and oligodendroglial gliomas. *Journal of Neuropathology and Experimental Neurology*, 64: 479-489.

Ohgaki H., Kleihues P. (2007) Genetic pathways to primary and secondary glioblastoma. *American Journal of Pathology*, 170:1445–1453.

Ohgaki H., Kleihues P. (2013) The definition of primary and secondary glioblastoma. *Clinical Cancer Research*, 19: 764-772.

O'Toole S. A., Sheppard B. L., McGuinness E. P., Gleeson N. C., Yoneda M., Bonnar J. (2003) The MTS assay as an indicator of chemosensitivity/resistance in malignant gynaecological tumours. *Cancer Detection and Prevention,* 27: 47-54.

Pace A., Lorenzo C. D., Guariglia L., Jandolo B., Carapella C. M., Pompili A. (2009) End of life issues in brain tumour patients. *Journal of Neuro-Oncology,* 91: 39-43.

Parsons D. W., Jones S., Zhang X., et al. (2008) An Integrated Genomic Analysis of Human Glioblastoma Multiforme. *Science,* 321: 1807.

Patel M., Vogelbaum M. A., Barnett G. H., Jalali R., Ahluwalia M. S. (2012) Molecular targeted therapy in recurrent glioblastoma: current challenges and future directions. *Expert Opinion on Investigational Drugs,* 21: 1247-1266.

Paul K., Hiroko O. (1999) Primary and secondary glioblastomas: From concept to clinical diagnosis. *Neuro Oncology,* 1: 44-51.

Prados M. D., Lamborn K. R., Chang S., Burton E., Butowski N., Malec M., Kapadia A., Rabbitt J., Page M. S., Fedoroff A., et al. (2006) Phase 1 study of erlotinib HCl alone and combined with Temozolomide in patients with stable or recurrent malignant glioma. *Neuro Oncology,* 8: 67–78.

Puck T. T., Marcus P. I. (1956) Action of x-rays on mammalian cells. *Journal of Experimental Medicine,*103: 653–666.

Purschke M., Rubio N., Held K. D., Redmond R. W. (2010) Phototoxicity of Hoechst 33342 in time-lapse fluorescence microscopy. *Photochemical and Photobiological Sciences,* 9: 1634-1639.

Rao E., Jiang C., Ji M., et al. (2012) The miRNA-17~92 cluster mediates chemoresistance and enhances tumour growth in mantle cell lymphoma via PI3K/AKT pathway activation. *Leukemia,* 26: 1064–1072.

Ravi M., Paramesh V., Kaviya S. R., Anuradha E., Solomon F. D. (2015) 3D cell culture systems: advantages and applications. *Journal of Cellular Physiology,* 230: 16-26.

Rich J. N., Reardon D. A., Peery T., et al. (2004) Phase II trial of gefitinib in recurrent glioblastoma. *Journal of Clinical Oncology*, 22: 133–142.

Riss T. L., Moravec R. A., Niles A. L., et al. (2013) *Cell Viability Assays*. In: Sittampalam GS, Coussens NP, Nelson H, et al., editors. Assay Guidance Manual. Bethesda (MD): Eli Lilly and Company and the National Center for Advancing Translational Sciences.

Ronald W., Matheny J., Martin L. A. (2009) Current Perspectives on Akt Akt-ivation and Akt-ions. *Experimental Biology and Medicine*, 234: 1264-1270.

Sancak Y., Thoreen C. C., Peterson T. R., Lindquist R. A., Kang S. A., Spooner E., Carr S. A., Sabatini D. M. (2007) PRAS40 is an insulin-regulated inhibitor of the mTORC1 protein kinase. *Molecular Cell*, 25: 903-915.

Santi S. A., Lee H. (2010) The AKT isoforms are present at distinct subcellular locations. *American Journal of Physiology - Cell Physiology,* 298: 580-591.

Sarbassov D. D., Guertin D. A., Ali S. M., Sabatini D. M. (2005) Phosphorylation and regulation of AKT/PKB by the rictor-mTOR complex. *Science*, 307: 1098-1101.

Sarker D., Workman P. (2007) Pharmacodynamic biomarkers for molecular cancer therapeutics. *Advances in Cancer Research*, 96: 213-268.

Sean C. T., Anton P. (2014) The Design of a Quantitative Western Blot Experiment. *BioMed Research International*. Article ID: 361590.

Shah R. R., Shah D. R. (2012) Personalized medicine: is it a pharmacogenetic mirage? *British Journal of Clinical Pharmacology*, 74: 698-721.

Shobu N., Jinmin Z., Klaus F., Matthias E., Anu S., Kevin J. T., Junying Y., Michael A. M. (1998) Activation and Cleavage of Caspase 3 in Apoptosis Induced by Experimental Cerebral Ischemia. *The Journal of Neuroscience*, 18: 3659–3668.

Stambolic V., Suzuki A., De P. J. L., Brothers G. M., Mirtsos C., Sasaki T., Ruland J., Penninger J. M., Siderovski D. P., Mak T. W. (1998) Negative regulation of PKB/AKT-dependent cell survival by the tumour suppressor PTEN. *Cell,* 95: 29–39.

Stupp R., Mason W. P., Van M. J., et al. (2005) Radiotherapy plus concomitant and adjuvant Temozolomide for glioblastoma. *New England Journal of Medicine*, 352: 987-996.

Todd M. P., Gillian N. K., Aik-Choon T., et al. (2013) Association of the epithelial-to-mesenchymal transition phenotype with responsiveness to the p21-activated kinase inhibitor, PF-3758309, in colon cancer models. *Frontiers in Pharmacology*, 4: 35.

Tokunaga E., Kataoka A., Kimura Y., et al. (2006) The association between AKT activation and resistance to hormone therapy in metastatic breast cancer. *European Journal of Cancer*, 42: 629–35.

Towbin H., Staehelin T., Gordon J. (1979) "Electrophoretic transfer of proteins from polyacrylamide gels to nitrocellulose sheets: procedure and some applications," *Proceedings of the National Academy of Sciences,* 76: 4350–4354.

Vacchelli E., Aranda F., Eggermont A., et al. (2014) Trial Watch: Tumour -targeting monoclonal antibodies in cancer therapy. *Oncoimmunology,* 3: e27048.

Van M. E. G., Hadjipanayis C. G., Norden A. D., Shu H. K., Wen P. Y., Olson J. J. (2010) Exciting New Advances in Neuro-Oncology: The Avenue to a Cure for Malignant Glioma. *CA: a cancer journal for clinicians*, 60: 166-193.

Vega-Avila E., Pugsley M. K. (2011) An Overview of Colorimetric Assay Methods Used to Assess Survival or Proliferation of Mammalian Cells. *Proceedings of the Western Pharmacology Society*, 54: 10-14.

Vermes I., Haanen C., Reutelingsperger C. (2000) Flow cytometry of apoptotic cell death. *Journal of Immunological Methods*, 243: 167–190.

Webb D. J., Brown C. M. (2013) Epi-Fluorescence Microscopy. *Methods in molecular biology*, 931:29-59.

Weisenthal L. M., Lippman M. E. (1985) Clonogenic and nonclonogenic in vitro chemosensitivity assays. *Cancer Treatment Reports*, 69: 615-632.

Weissleder R. (2002) Scaling down imaging: molecular mapping of cancer in mice. *Nature reviews*, 2: 11-18.

Weller M., Cloughesy T., Perry J. R., Wick W. (2013) Standards of care for treatment of recurrent glioblastoma--are we there yet? *Neuro Oncology,* 15: 4-27.

Wen-I W., Walter C. V., Hillary L., Faith P. D., Guy P. A. V., Barbara J. B. (2010) Crystal Structure of Human AKT1 with an Allosteric Inhibitor Reveals a New Mode of Kinase Inhibition. *PLoS One*, 5: e12913.

Winograd-Katz S. E., Levitzki A. (2006) Cisplatin induces PKB/AKT activation and p38 (MAPK) phosphorylation of the EGF receptor. *Oncogene*, 25: 7381–7390.

Xin H., Khalil C., Steven N. K. (2012) Glioblastoma cell line-derived spheres in serum-containing medium versus serum-free medium: A comparison of cancer stem cell properties. *International Journal of Oncology*, 41: 1693-1700.

Xing D., Orsulic S. (2005) A genetically defined mouse ovarian carcinoma model for the molecular characterization of pathway-targeted therapy and tumour resistance. *Proceedings of the National Academy of Sciences*, 102: 6936–6941.

Yang J., Cron P., Thompson V., Good V. M., Hess D., et al. (2002) Molecular mechanism for the regulation of protein kinase B/AKT by hydrophobic motif phosphorylation. *Molecular Cell*, 9: 1227–1240.

Zoncu R., Efeyan A., Sabatini D. M. (2011) mTOR: From growth signal integration to cancer, diabetes and ageing. *Nature Reviews Molecular Cell Biology*, 12: 21–35.